

1 Article type: Original Articles

2 **The ALIOS diet in male and female rodents recapitulates the clinical and transcriptomic**  
3 **features of NAFLD and NASH**

4 Shelley E Harris<sup>1</sup>, Toryn M Poolman<sup>1</sup>, Anastasia Arvaniti<sup>1,2</sup>, Roger D Cox<sup>3</sup>, Laura L  
5 Gathercole<sup>1,2</sup> and Jeremy W Tomlinson<sup>1</sup>

6

7 1. Oxford Centre for Diabetes, Endocrinology and Metabolism, NIHR Oxford Biomedical  
8 Research Centre, University of Oxford, Churchill Hospital, Oxford, UK, OX3 7LE, UK

9 2. Department of Biological and Medical Sciences, Oxford Brookes University, Oxford, OX3  
10 OBP, UK.

11 3. Mammalian Genetics Unit, Medical Research Council Harwell Institute, Oxford, OX11 0RD,  
12 UK

13

14 **Abbreviated title:** The ALIOS diet recapitulates NASH in mice

15

16 **Correspondence author:** Professor Jeremy Tomlinson: [Jeremy.tomlinson@ocdem.ox.ac.uk](mailto:Jeremy.tomlinson@ocdem.ox.ac.uk).

17 Oxford Centre for Diabetes, Endocrinology and Metabolism, NIHR Oxford Biomedical  
18 Research Centre, University of Oxford, Churchill Hospital, Oxford, UK, OX3 7LE, UK

19

20 **Author contribution:** Conceptualisation S.E.H, L.L.G, R.D.C and J.W.T; Methodology S.E.H,

21 T.M.P, A.A, L.L.G; Investigation S.E.H, T.P. L.L.G; Writing S.E.H and J.W.T; Supervision, J.W.T.;

22 Funding Acquisition, J.W.T.

23 **Word Count:** 4714 **Figures:** 8 **Tables:** 4

24 **Abbreviations:** ALT: alanine aminotransferase. ALP: alkaline phosphatase. ALIOS: American  
25 lifestyle induced obesity syndrome diet. AST: aspartate aminotransferase. HCC:

26 hepatocellular carcinoma. HDL: high-density-lipoprotein. HFD: high fat diet. LDL: low-density  
27 protein. NAFLD: non-alcoholic fatty liver disease. NASH: non-alcoholic steatohepatitis. NC:  
28 normal chow. TAG: triacylglycerols.

29

30

31

32

33

34

35

36

37

38

39

40

41

42

43

44

45

46

47

48

49

50

51

52 **Abstract:** 226 words

53 **Background & Aims:** The pathogenesis of non-alcoholic fatty liver disease (NAFLD) and the  
54 progression to non-alcoholic steatohepatitis (NASH) and increased risk of hepatocellular  
55 carcinoma (HCC), remain poorly understood. Additionally, there is increasing recognition of  
56 the extra-hepatic manifestations associated with NAFLD and NASH. We demonstrate that  
57 intervention with the American lifestyle induced obesity syndrome diet (ALIOS) in male and  
58 female mice recapitulates many of the clinical and transcriptomic features of human NAFLD  
59 and NASH. **Methods:** Male and female C57BL/6N mice were fed either normal chow (NC) or  
60 ALIOS from 11 to 52-weeks and underwent comprehensive metabolic analysis throughout  
61 the duration of the study. **Results:** From 26-weeks, ALIOS-fed mice developed features of  
62 hepatic steatosis, inflammation and fibrosis. ALIOS-fed mice also had an increased incidence  
63 of hepatic tumours at 52-weeks compared to those fed NC. Hepatic transcriptomic analysis  
64 revealed alterations in multiple genes associated with inflammation and tissue repair in  
65 ALIOS-fed mice. Ingenuity Pathway Analysis confirmed dysregulation of metabolic pathways  
66 as well as those associated with liver disease and cancer. In parallel the development of a  
67 robust hepatic phenotype, ALIOS-fed mice displayed many of the extra-hepatic  
68 manifestations of NAFLD including hyperlipidaemia, increased fat mass, sarcopaenia and  
69 insulin resistance. **Conclusions:** The ALIOS diet in mice recapitulates many of the clinical  
70 features of NAFLD and therefore represents a robust and reproducible model for  
71 investigating the pathogenesis of NAFLD and its progression.

72

73 **New and Noteworthy:** NAFLD affects 30% of the general population and can progress to  
74 NASH and potentially hepatocellular carcinoma. Pre-clinical models rely on mouse models  
75 which often display hepatic characteristics of NAFLD, but rarely progress to NASH and  
76 seldom depict the multi-system effects of the disease. We have conducted comprehensive

77 metabolic analysis of both male and female mice consuming a western diet of trans-fats and  
78 sugar, focussing on both their hepatic phenotype, but also the extra-hepatic manifestations.

79

80 **Key words:** Non-alcoholic fatty liver disease, non-alcoholic steatohepatitis, diet,  
81 transcriptome.

82

83

84

85

86

87

88

89

90

91

92

93

94

95

96

97

98

99

100

101

102

103 **Introduction**

104 Non-alcoholic fatty liver disease (NAFLD) is the hepatic manifestation of metabolic syndrome  
105 and is the most common form of liver disease in the western world (2, 25). NAFLD currently  
106 affects around 30% of the normal population and rises to 80% in patients with obesity and  
107 type 2 diabetes (24, 25). It is a spectrum disease, ranging from simple steatosis through to  
108 the necro-inflammatory disease, non-alcoholic steatohepatitis (NASH). Development of  
109 NASH subsequently increases the risk of fibrosis and cirrhosis and eventually, hepatocellular  
110 carcinoma (HCC) (51, 52). Recent evidence supports the concept that NAFLD is a multi-  
111 systemic condition impacting upon a variety of organs and systems (5, 48) and is associated  
112 with multiple extra-hepatic clinical features, including insulin resistance, hyperlipidaemia  
113 and sarcopenia.

114

115 Pre-clinical mouse models of NAFLD and NASH typically rely on genetic manipulation,  
116 hepatic cytotoxic injury or formulated dietary extremes (11, 16, 29). Although some of these  
117 models exhibit the histological features of NAFLD, they rarely progress to NASH or HCC and  
118 therefore do not reflect the mechanisms of the human disease. Commonly used genetic  
119 models of obesity, the leptin-deficient (*ob/ob*) mouse and leptin receptor-deficient (*db/db*)  
120 mouse, have excess hepatic fat deposition, but do not develop NASH or HCC (1, 11, 36),  
121 most likely because leptin is involved in regulating inflammation and fibrosis. In addition,  
122 models using high fat diet (HFD; 60% fat) cause simple steatosis but do not progress to NASH  
123 or develop hepatic injury (11, 34). Fructose has been shown to be a driver of hepatic *de novo*  
124 lipogenesis (43), however, fructose only dietary interventions often fail to induce  
125 dyslipidemia, hepatic steatosis and inflammation (28, 41). Previous studies have utilised  
126 “fast food” diets (7, 22), which contain 40% fat (12% from saturated fat) with the addition of  
127 fructose in drinking water, though these studies progress to characteristic NASH, they  
128 seldom highlight the extra-hepatic features of the disease and sexual dimorphism has not

129 been explored. Alternative models use hepatic toxins to drive liver injury. These commonly  
130 include carbon tetrachloride with which animals develop hepatic histological features of  
131 NASH and fibrosis from as early as 8 weeks, but often do not present with other clinical  
132 features of NASH such as weight gain and insulin resistance (47). Diethylnitrosamine is able  
133 to induce HCC but does so without the progression from NAFLD and NASH (19).  
134 Furthermore, the use of genetic manipulation, in combination with toxins and HFD in  
135 generating models of NAFLD poses questions as to the relevance and similarity to human  
136 NAFLD and NASH.

137 The American lifestyle-induced obesity syndrome (ALIOS) mouse model is a dietary  
138 intervention based on the nutritional content of commonly consumed fast foods of the  
139 western world (46). Mice are fed high fat chow (45%), including trans fats, with high fructose  
140 corn syrup added to the drinking water; animals become obese, insulin resistant and  
141 develop hepatic steatosis with a necro-inflammatory response (10, 46). When aged to 12  
142 months, mice fed ALIOS also develop NASH driven HCCs (10). To date, studies using ALIOS  
143 have only treated male mice, therefore the effects of ALIOS on female metabolism is entirely  
144 unexplored. In addition, with the increasing evidence suggesting the importance of the  
145 extra-hepatic impact of NAFLD, models that can accurately replicate a clinical condition are  
146 likely to be more highly informative, both with respect to natural history, but also the  
147 potential impact of intervention. In the published literature, studies have largely focused on  
148 the hepatic phenotype associated with the ALIOS diet, and its multi-system impact has not  
149 been evaluated in detail.

150

151 We have therefore conducted a comprehensive metabolic analysis of both male and female  
152 mice consuming either an ALIOS diet or standard chow from 11 to 52 weeks of age,  
153 focussing on both their hepatic phenotype, but also the extra-hepatic manifestations.

154

155  
156  
157  
158

## **Methods**

### 159 *Mouse husbandry*

160 Male and female C57BL/6NTac mice were kept and studied in accordance with UK Home  
161 Office legislation and local ethical guidelines issued by the Medical Research Council  
162 (Responsibility in the Use of Animals for Medical Research, July 1993; home office license  
163 30/3146). All procedures were conducted in accordance with the Animals (Scientific  
164 Procedures) Act 1986 Amendment Regulations 2012 (SI 4 2012/3039). Mice were kept under  
165 controlled light (light 7am–7pm, dark 7pm–7am), temperature ( $21\pm 2^{\circ}\text{C}$ ) and humidity  
166 ( $55\pm 10\%$ ) conditions. They had free access to water (9–13 ppm chlorine) and were fed *ad*  
167 *libitum* on a commercial diet (SDS Rat and Mouse No. 3 Breeding diet, RM3) until 10 weeks  
168 of age when they were then transferred to a control (NC; SDS Rat and Mouse No. 3 Breeding  
169 diet, RM3, Essex, UK) or ALIOS diet (D06031302, Research Diets, USA and TD06415 with  
170 hydrogenated vegetable fats, Envigo, USA, [45% fat of which 30% is trans-fat] with 55%  
171 fructose:45% glucose in drinking water) for 26- or 52-weeks before culling by cervical  
172 dislocation and tissue analysis.

173

### 174 *Experimental design*

175 Cohorts of male and female mice were bred for longitudinal metabolic phenotyping tests  
176 (26w cohort: NC males n=12, ALIOS males n=15, NC females n=15, ALIOS females n=15. 52w  
177 cohort: (NC males n=17, ALIOS males n=12, NC females n=15, ALIOS females n=15). Mice  
178 were housed in single sex groups across multiple litters and were not randomised into  
179 groups. Animal IDs and diets were recorded on the cages and were not blinded to the  
180 operator carrying out the animal procedure although subsequent tests only include animal

181 ID information. Sample size estimates were based on previous experience of mouse models  
182 in which relevant traits were measured (9, 10, 38).

183

#### 184 *Body weight and composition*

185 Body weight was measured weekly in the morning using average weights (g) calculated by  
186 Adventure Pro balances (Ohaus, US). Fat and lean mass was assessed by Dual-energy X-ray  
187 absorptiometry (DEXA) at 17, 25, 39 and 51 weeks of age.

188

#### 189 *Calorimetry*

190 Calorimetry data was collected in a PhenoMaster system (TSE Systems, Germany) at 14, 25,  
191 36 and 48 weeks of age. Mice were kept under controlled light (light 7am–7pm, dark 7pm–  
192 7am), temperature ( $21\pm 2^\circ\text{C}$ ) and humidity ( $55\pm 10\%$ ) conditions. They had free access to  
193 water (9–13 ppm chlorine) and were fed *ad libitum*.  $\text{O}_2$  consumption ( $\text{VO}_2$ ),  $\text{CO}_2$  production  
194 ( $\text{VCO}_2$ ) and respiratory exchange ratio (RER ( $\text{VCO}_2/\text{VO}_2$ ), an estimate of fuel usage) were  
195 calculated and recorded electronically over 12 hours for each mouse. Total locomotor  
196 activity (measured by x, y, and z axis infrared beam breaks) and diet consumption were also  
197 recorded electronically for each mouse. Data were collected at 3 to 4 time points each hour.

198

#### 199 *Intraperitoneal glucose tolerance test (ipGTT)*

200 Glucose tolerance was assessed at 15, 25, 37 and 49 weeks of age. Mice were fasted  
201 overnight for 16 hours then injected intraperitoneally with 20% glucose solution (2g  
202 glucose/kg body weight; Sigma, Dorset, UK). Blood was sampled from the tail vein and  
203 glucose concentration measured at t=0, 15, 30, 60, and 120 minutes (Alphatrak, Abbott, UK).  
204 Insulin concentrations at t=0, 60 and 120 minutes were determined by ELISA (Crystal Chem,  
205 USA). The homeostasis model assessment of insulin resistance (HOMA-IR) index was  
206 calculated as [fasting glucose (mmol/L) x fasting insulin ( $\mu\text{U/ml}$ )/22.5] (13).



207

208

209

210 *Intraperitoneal insulin tolerance test (ipITT)*

211 Insulin tolerance was assessed at 25, 37 and 49 weeks. Mice were fasted for 4-5 hours then  
212 injected intraperitoneally with insulin at a concentration of 0.75 or 1.25 IU/kg for females  
213 and males, respectively (Hypurin Bovine Insulin). Blood was sampled from the tail vein and  
214 glucose concentration measured at t=0, 15, 30, 45 and 90 minutes (Alphatrak, Abbott, UK).

215

216 *Blood biochemistry*

217 At termination, mice were anaesthetised with isoflurane and blood collected *via* retro-  
218 orbital bleed. Samples were kept on ice then centrifuged for 10 minutes at 8,000 x g at room  
219 temp. Alkaline phosphatase (ALP), alanine aminotransferase (ALT), aspartate  
220 aminotransferase (AST), cholesterol, high-density-lipoprotein (HDL), low-density-lipoprotein  
221 (LDL), triglycerides, free fatty acids and bilirubin were determined from plasma on an AU680  
222 Clinical Chemistry Analyser (Beckman Coulter, High Wycombe, UK). Creatinine was analysed  
223 using a colorimetric kit appropriate for mouse serum (Cayman Chemicals, Cambridge, UK).

224

225 *Tissue biochemistry*

226 Hepatic triacylglycerol content was measured on an AU480 Clinical Chemistry Analyser  
227 (Beckman Coulter, High Wycombe, UK), from a homogenate of frozen liver tissue (100mg  
228 in 500µl of PBS/0.1% Triton-X).

229

230 *Tissue Histology*

231 Liver tissue was fixed in 4% (vol/vol) buffered formaldehyde and samples were subsequently  
232 paraffin-embedded and 5-µm sections prepared on a microtome. Sections were stained with

233 H&E and viewed at 200x magnification. Inflammation score was determined by counting the  
234 number of inflammatory foci in 5 fields of view over 3 sections from each mouse liver (20,  
235 23) and the average scored as follows: no foci = 0, <2 per field of view = 1, 2-4 per field of  
236 view = 2, >4 per field of view = 3. A foci was determined as a cluster of 5 or more  
237 inflammatory cells. Percentage of hepatic fibrosis was determined by staining 3 sections  
238 from each mouse liver with Sirius Red and quantifying percentage of positive staining over 6  
239 fields of view by ImageJ (NIH, USA; <http://rsb.info.nih.gov/ij>).

240

#### 241 *Immunohistochemistry*

242 Immunohistochemistry was performed on wax embedded liver sections (5µm). Briefly,  
243 sections were dewaxed and rehydrated before incubation with antibodies against glutamine  
244 synthetase (5µg/ml; Millipore, Watford, UK) and Sox9 (1µg/ml; Millipore) after heat  
245 induced antigen retrieval. Bound primary antibody was detected using a peroxidase-  
246 conjugated secondary antibody (Dako) with visualisation using 3,3- diaminobenzidine  
247 (SigmaFast, Sigma, Dorset, UK). For negative control samples, non-immune goat's serum  
248 replaced primary antibodies.

249

#### 250 *Protein extraction and immunoblotting*

251 Total protein was extracted from whole liver tissue using RIPA buffer (150mM NaCl, 1.0%  
252 IGEPAL® CA-630, 0.5% sodium deoxycholate, 0.1% SDS, and 50 mM Tris, pH 8.0; Sigma,  
253 Dorset, UK), with protease and phosphatase inhibitor cocktail (ThermoFisher Scientific,  
254 Loughborough, UK). Protein concentrations were measured using a BCA protein  
255 quantification kit according to the manufacturer's protocol (Thermo scientific). Primary  
256 Col1A1 (Cell Signalling Technology, Leiden, The Netherlands) and secondary antibodies from  
257 Dako (Agilent Technologies, Santa Clara, USA) were used at a dilution of 1/1000 and 1/2000  
258 respectively. Bands were visualised with ECL (Pierce Thermo Fisher Scientific) and

259 ChemiDocXS imager (Biorad, Watford, UK). Bands were quantified by densitometry and  
260 normalised to total protein using ImageJ (NIH, Bethesda, MD, <http://rsb.info.nih.gov/ij>).

261

262

### 263 *RNA sequencing*

264 Total liver RNA was extracted using Tri-Reagent (Sigma, Dorset, UK). Concentration was  
265 determined spectrophotometrically at OD260 on a Nanodrop spectrophotometer (Thermo  
266 Scientific, Hemel Hempstead, UK) and quality checked on a 2100 Bioanalyzer system (Agilent  
267 Technologies, Stockport, UK). Only samples with RNA integrity numbers >7 were used for  
268 analysis. cDNA was generated from total RNA using first oligodT and subsequently random  
269 priming using the TruSeq Stranded mRNA HT Sample Prep Kit for Illumina (according to  
270 manufacturer's instructions). The prepared libraries were QC'ed and multiplexed, followed  
271 by pair-end sequencing (75bp) over one lane of a NextSeq 75SR flow cell (Illumina,  
272 Cambridge, UK) to a total depth of 130 million read pairs on the Illumina NextSeq 500  
273 platform (Illumina, Cambridge, UK). Reads were mapped with Stampy (31) on default  
274 settings with GRCm38/mm10 as genome reference and bam files merged using bamtools.  
275 Gene level read counts for all protein-coding RNA transcripts present in refGene mm10 were  
276 quantified in a strand-specific manner using FeatureCounts from the Subread package  
277 v1.6.0. Differential expression analysis was performed using DESeq2 (30). Differentially  
278 expressed genes (DEGs) were reported for  $q \leq 0.05$  and fold change of 2 or  $q \leq 0.1$ . Statistical  
279 significance was determined by unpaired parametric t-test and differentially regulated genes  
280 were defined by a false discovery rate (Benjamini-Hochberg method) adjusted p-value < 1%.  
281 The online bioinformatics tools Metascape ([metascape.org](http://metascape.org)) and Enrichr  
282 (<http://amp.pharm.mssm.edu/Enrichr/>) were used for enrichment analysis of the DE genes.  
283 Ingenuity Pathway Analysis (IPA; Ingenuity Systems Inc., USA) was used to examine  
284 biological functions and disease and functional relationships between gene networks.

285

286 *Bioinformatic Data Analysis*

287 RNA-seq data was downloaded from NCBI (GSE126848). Gene counts  
288 (GSE126848\_Gene\_counts\_raw.txt) and sample identification were determined from the  
289 series matrix (GSE126848\_series\_matrix.txt). The clinical characteristics of patients are  
290 described in Supp. Table 1 (<https://doi.org/10.6084/m9.figshare.12666860>). Gene symbols  
291 were converted from Ensembl ID using (org.Hs.eg.db v3.11.4). Differential gene expression  
292 was determined using EdgeR (3.11). As the human NASH dataset contained 12 male samples  
293 and 4 female samples, RNA-seq libraries from female samples were removed. All remaining  
294 samples were included (Normal weight, obese, NAFLD and NASH), low counts were removed  
295 (CPM>0.25 in 2 libraries), and differential expression for NASH vs Normal weigh samples  
296 were determined, this gave 3152 down regulated and 3491 up regulated genes(using EdgeR  
297 glmLRT). Differentially expressed genes from male mice (ALIOS vs normal chow, 2153 down  
298 regulated and 2865 up regulated) were used to convert to human symbols. Mouse Gene  
299 symbols (5018) were converted using the package BiomartR (v2.440). 4701 genes were  
300 matched between human and mouse. NASH regulated genes were then compared to ALIOS  
301 regulated genes. A list of 2052 genes were identified as overlapping, with significance  
302 determined using Fisher's Exact Test (a Venn diagram was produced, using the  
303 ggVennDiagram R package). The overlapping genes were used for pathway analysis and  
304 plotted on heatmaps (using ggplot2). The top 30 significant genes (sorted by false discovery  
305 rate) in the NASH dataset were extracted. LogCPM counts were used for each heatmap,  
306 each dataset (mouse and human) was scaled separately before plotting.

307

308 *Statistics*

309 Data are presented as mean  $\pm$  standard error. Data analysis was performed using Graphpad  
310 Prism software (Graphpad Software Inc, La Jolla, USA) and considered statistically significant

311 at  $p < 0.05$ . Normality was assessed using the Shapiro-Wilk test. Two-tailed, unpaired t-tests  
312 were used to compare differences in the mean between diets within each sex. Mann-  
313 Whitney tests were used with datasets of non-parametric distributions. For data collected  
314 across time, repeated measure two-way analysis of variance (ANOVA) was used.

315

## 316 **Results**

### 317 *Male and female mice fed ALIOS have progressive weight gain and increased fat mass*

318 Weight gain was greater in both male and female ALIOS fed mice and body weight continued  
319 to rise throughout the study, from the onset of ALIOS at 11-weeks until 52-weeks (Fig 1A,B).  
320 From 15-weeks onwards, DXA analysis confirmed that ALIOS fed mice of both sexes had an  
321 increase in fat mass compared to normal chow controls (Fig. 1C,D). Interestingly, at 15- and  
322 37-weeks female mice also displayed a decrease in lean mass. There was no change in lean  
323 mass in the male mice throughout the duration of the study.

324

325 At 26-weeks, male ALIOS fed mice had increased fat pad weights across all depots compared  
326 to NC controls. However, by 52-weeks, gonadal fat was the only enlarged depot (Fig.1E).  
327 ALIOS fed female mice had increased fat depots at both 26- and 52-weeks compared to NC  
328 controls (Fig.1F). Consistent with increased lipid storage, ALIOS fed male and female mice  
329 had increased serum levels of total, HDL and LDL cholesterol from 25-weeks onwards (Table  
330 1). Circulating levels of triacylglycerols (TAG) and free fatty acids (FFA) were significantly  
331 decreased in ALIOS fed mice compared to NC controls, at 52-weeks and from 25-weeks in  
332 males and females, respectively (Table 1). In addition, data from metabolic cage  
333 experiments revealed that male mice were more sedentary than females and that ALIOS fed  
334 mice had reduced total activity compared to NC controls (Supp. Tables 2 and 3). As  
335 expected, respiratory exchange ratios were reduced in male and female ALIOS fed mice,  
336 indicating increased fat catabolism for energy production (Supp. Tables 2 and 3).

337

338 At 26-weeks, kidney size was reduced in both male and female mice and quadriceps weight  
339 decreased in female mice only (Supp. Fig.1). By 52-weeks, male ALIOS fed mice had  
340 decreased heart, quadricep and testes mass compared to those fed NC, alongside an  
341 increase in spleen mass (Supp. Fig.1A). Serum creatinine levels were elevated in male ALIOS  
342 fed mice compared to NC controls at 52-weeks (Table 2). Female ALIOS fed mice mirrored  
343 the changes in quadricep and spleen mass seen in the males and also had a reduction in  
344 kidney mass (Supp. Fig.1B) and increase in serum creatinine (Table 2).

345

346 *ALIOS fed mice have normal glucose tolerance but are insulin resistant.*

347 There was no difference in glucose tolerance in ALIOS fed male mice throughout the  
348 duration of the study (Fig. 2A). In females, glucose tolerance was impaired at 25- and 37-  
349 weeks in ALIOS mice, although by 49-weeks, there was no difference in comparison with NC  
350 fed animals (Fig.2B). However, the ALIOS diet increased serum insulin levels in response to  
351 the glucose bolus, in both male and female mice, compared to NC controls consistent with  
352 the development of insulin resistance (Fig. 2E,F & Supp. Fig. 2).

353 Further evidence of insulin resistance was obtained from insulin tolerance testing; in both  
354 male and female ALIOS fed mice from 37-weeks onwards, there was an impaired glycaemic  
355 response to intraperitoneal insulin injection (Fig.3A,B & Supp. Fig. 3). There was no change  
356 in insulin sensitivity at 25-weeks in ALIOS fed mice of either sex. The HOMA-IR was increased  
357 in both male and female ALIOS-fed mice from 15-weeks onwards (Fig. 3C,D).

358

359 *ALIOS drives hepatic steatosis and inflammation*

360 Liver to body weight mass was increased in both male and female ALIOS fed mice compared  
361 to NC at 26- and 52-weeks (Fig.4A,B). Additionally, hepatic triglyceride was elevated in ALIOS  
362 fed mice of both sexes at 26-weeks and in male mice at 52-weeks (Fig.4C,D). Histological

363 examination of all ALIOS livers identified steatosis, with evidence macro- and micro-vesicular  
364 lipid droplets and ballooning of hepatocytes (Fig.4E,F). ALIOS fed male and female mice had  
365 altered expression of genes associated with lipid metabolism (*Srebf1, Elovl3, Lpl*; Fig.4G,H)  
366 insulin signalling (*Irs1, G6pc, Glut4, Pck1*; Fig.4I,J).

367

368 At 26-weeks, male ALIOS fed mice displayed no change in histologically determined  
369 inflammation score, however this was increased by 52-weeks (Fig.5A). In contrast, female  
370 mice fed ALIOS had an increased inflammation score from 26-weeks which persisted to 52-  
371 weeks (Fig.5B). ALIOS fed male and female mice had increased hepatic expression of genes  
372 involved in inflammation, including macrophage infiltration, (*Tnf, Ccl2, Cd68, f4/80*; Fig 5C,D)  
373 compared to NC fed mice at 52-weeks.

374

375 *Male ALIOS fed mice have increased incidence of fibrosis and HCCs*

376 ALIOS fed mice of both sexes, had elevated serum levels of ALT and AST from 26-weeks  
377 onwards, and continued to rise throughout the duration of the study suggesting hepatocyte  
378 damage and the presence of fibrosis (Table 2); the AST/ALT ratio was decreased in ALIOS fed  
379 mice compared to controls, which is suggestive of NAFLD. Serum levels of bilirubin, however,  
380 were unchanged in ALIOS fed mice compared to NC controls (Table 2). Hepatic fibrosis  
381 percentage was increased in male ALIOS fed mice compared to NC controls at 26- and 52-  
382 weeks (Fig.6A), while in female ALIOS fed mice percentage fibrosis was only increased at 52-  
383 weeks (Fig.6B). Both ALIOS fed male and female mice had increased hepatic expression of  
384 genes associated with cell adhesion (*Col1a1, Col1a2, Dpt, Lum*; Fig.6C,D) as well as increased  
385 protein levels of collagen type 1 (*Col1a1*; Fig.6E,F).

386

387 Advanced fibrotic disease increases the risk of HCC; male mice fed ALIOS had an increased  
388 frequency of macroscopic liver growths (NC: 5.8%, ALIOS: 25%,  $P<0.05$ ). There was no

389 evidence of liver lesions in female ALIOS fed mice. The lesions were associated with  
390 compressed adjacent non-tumour tissue, though there appeared to be no invasion of blood  
391 vessels or surrounding liver tissue (Fig.6I). Histological assessment revealed that the lesions  
392 were composed of atypical hepatocytes with increased nuclear to cytoplasmic ratios, as well  
393 as some multinucleated cells (Fig.6J). As there was no obvious evidence of invasion to  
394 confirm malignancy, characterisation was performed using HCC markers commonly used in  
395 mice and humans. Sox9 is a marker of hepatic stem cell activation previously implicated in  
396 tumour pathogenesis (18, 37) and labelling was positive in the nucleus of the atypical  
397 hepatocytes of only 1/3 lesions (Fig.6K). Glutamine synthetase (GS) has previously been  
398 used to determine well differentiated HCCs from pre-malignant tumours in human liver (10,  
399 37, 49). Diffuse GS was also only present in 2/3 ALIOS lesions (Fig.6L).

400

#### 401 *ALIOS diet alters the hepatic transcriptome in male and female mice*

402 Clustering of NC and ALIOS of the top 100 DEGs revealed two distinct groups between NC  
403 and ALIOS with almost no overlapping (Fig.7A,B). In male mice, 5018 genes were  
404 differentially expressed between NC and ALIOS, 2153 were down-regulated and 2865 were  
405 up-regulated (Table 3). Within the top 10 up-regulated genes, three were associated with  
406 the major histocompatibility complex (MHC). Gene ontology analysis highlighted that the  
407 most up-regulated genes were associated with reorganisation of cellular structures and  
408 collagen binding as well as inflammatory and immune response (Fig.7C). The down-  
409 regulated genes were mostly clustered to biological pathways involved in metabolism and  
410 protein processing (Fig.7D). In line with these findings, the top diseases and functions  
411 captured in IPA included cancer, organismal injury and endocrine disorders (Table 4). The  
412 top toxicology lists by IPA included liver necrosis and hepatic fibrosis, as well as NRF2-  
413 mediated Oxidative Stress Response.



414 In livers of ALIOS fed female mice, a total of 4222 genes showed differential expression;  
415 2350 genes were up- and 1871 were down-regulated (Table 3). The most up-regulated genes  
416 were associated exclusively with inflammatory processes (Fig.7E), while down-regulated  
417 genes, as in male mice, clustered to metabolic processes (Fig.7F). Similarly, the top diseases  
418 and functions identified by IPA included cancer, injury and endocrine disorders (Table 4).  
419 The top toxicology lists as determined by IPA included hepatic fibrosis, liver necrosis and  
420 steatosis.

421

422 To identify DEGs associated with NASH in humans, published RNAseq data from liver  
423 biopsies of patients with NASH was re-analysed alongside biopsies from patients with  
424 normal bodyweight. A total of 4558 human DEGs were identified. Comparative analysis  
425 revealed that 2052 (22.5%) genes were shared by the human NASH patients and male ALIOS  
426 fed mice (Fig.8A). Out of the 2052 common genes, 1018 were up-regulated and 1034 were  
427 down-regulated. The clustering of the top 30 overlapped genes revealed similarities  
428 between livers of ALIOS fed mice and human NASH liver biopsies (Fig.8B). Genes associated  
429 with lipid metabolism (Fig.8C; LPL), insulin signalling (G6PC, PCK1), inflammation (TNFA1P3,  
430 CCL2, CXCR4) and cell adhesion (DPT, LUM, COL1A1) were among those that which were  
431 altered in both human NASH and ALIOS fed male mice. Additionally, gene ontology analysis  
432 revealed that the top 100 shared genes were enriched in pathways associated with immune  
433 response, metabolic processes and cell migration (Fig.8D), confirming that most of the genes  
434 and pathways conserved between the ALIOS mouse model and human NASH are associated  
435 with inflammation and fibrosis.

436

#### 437 **Discussion**

438 NAFLD is rapidly becoming the most common cause for liver transplantation. However,  
439 there are aspects of its pathology that remain poorly understood, and informative pre-

440 clinical models that accurately reflect the clinical condition, particularly its natural history  
441 and progression, can provide valuable mechanistic insight. In this study, we have shown that  
442 male and female mice fed the ALIOS diet for 52-weeks develop a classical and reproducible  
443 hepatic phenotype (including elevated liver chemistry, histological features of NASH and the  
444 development of HCC). However, we also have shown that they develop many of the extra-  
445 hepatic features associated with NAFLD including, increased fat mass, sedentary behaviour,  
446 abnormal circulating lipid profiles, insulin resistance, and sarcopenia. Kidney weights were  
447 reduced and serum creatinine levels were elevated in ALIOS fed mice. Recent reports have  
448 highlighted the association between NAFLD and renal dysfunction in humans (32, 44).  
449 Furthermore, we have highlighted the differential gene expressions in ALIOS fed mice  
450 compared to NC controls that may prove highly informative in enhancing our understanding  
451 of the pathogenesis of NAFLD.

452

453 Male and female ALIOS fed mice had increased bodyweight from as early as 11-weeks,  
454 driven by increased fat mass. Of note, bodyweights in female ALIOS-fed mice continue to  
455 increase at 52-weeks and do not plateau, contrasting with male ALIOS-fed mice. It's  
456 interesting to speculate that this sexually dimorphic trajectory might extend to the liver in  
457 that the females might also develop HCCs as seen in the males, if left for longer than one  
458 year. Unfortunately we did not extend our observations beyond one year in either sex.  
459 Detailed body composition analysis has not been undertaken in this model previously and  
460 we have been able to show increased fat depot mass, with additional evidence for reduced  
461 skeletal muscle (quadriceps mass). This finding mirrors the sarcopenia that is associated with  
462 NAFLD (8); Koo *et al.* (21), reported that sarcopenia was present in 17.9% and 35% of  
463 patients with NAFLD and NASH, respectively and was associated with significant fibrosis and  
464 insulin resistance (21). Previous studies have demonstrated abnormal glucose handling and  
465 insulin resistance in mice fed the ALIOS diet (10, 46) and we have now shown that this

466 persists throughout the duration of the intervention (at least to 52-weeks).Total (including  
467 both LDL and HDL) cholesterol became elevated soon after the commencement of the diet,  
468 although circulating triglyceride levels were lower in both male and female mice on the  
469 ALIOS diet at 52 weeks. It is possible that this may reflect impaired hepatic lipid export  
470 therefore contributing to increased hepatic triglyceride accumulation.

471

472 The liver phenotype that we have observed is similar to that which has been described  
473 previously (10, 46) and we have now extended the detailed phenotyping to 52-weeks  
474 duration. At 26-weeks steatosis is predominately periportal, but, by 52-weeks, macro- and  
475 micro-vesicle steatosis has extended to the centrilobular region. The development of micro-  
476 vesicular steatosis may be linked to increased disease progression; in humans micro  
477 vesicular steatosis from liver biopsies correlated positively with increased NASH diagnosis  
478 and advanced fibrosis (45). By 52-weeks, there was clear evidence of hepatic fibrosis in both  
479 male and female mice. In male mice, the ALIOS diet was associated with an increased  
480 incidence of liver tumours as we have shown previously (10). However, female mice  
481 appeared to be completely protected from this. Male predisposition to HCC is well described  
482 (15, 17, 35) and in this regard, the ALIOS model appears to replicate clinical findings. The  
483 atypical hepatocytes seen in the liver lesions from ALIOS fed male mice are a recognised  
484 feature of human hepatic tumours. Unfortunately, there is no established panel of murine  
485 HCC markers that are comparable to human (40); the use of IHC markers was variable across  
486 different lesions from different mice. Glutamine synthetase is a target gene of  $\beta$ -catenin,  
487 and its overexpression is associated with mutations of  $\beta$ -catenin and/or activation of its  
488 pathway. In mice, hepatocellular tumours express differing levels of GS depending on the  
489 type of mutation within the neoplasm (40).

490

491 Unbiased transcriptomic analysis provides a powerful tool with which to interrogate the  
492 processes that drive NAFLD to the more advanced disease stages. Our analysis  
493 demonstrated increased mRNA expression of pro-inflammatory cytokines (*Tnf*, *Ccl2*, *Ccl3*) in  
494 male and female ALIOS fed mice, as well as markers of macrophage (*Cd68*, *Cd40*, *F4/80*) and  
495 Kupffer cell infiltration. Endorsing these observations, a direct comparison of the  
496 transcriptome from ALIOS fed male mice with publically available RNAseq data from biopsies  
497 of patients with NASH highlights a significant overlap of genes associated with NAFLD and  
498 NASH. Moylan *et al.*, (33) reported a 64-gene profile of up-regulated genes in severe NAFLD  
499 in humans, which included genes associated with inflammation, cell adhesion and liver  
500 progenitor cells. These pathways are believed to be crucial in the progression from steatosis  
501 to NASH as well as to the development of HCC (11, 12), further validating the ALIOS diet as a  
502 good model of the full NAFL spectrum of disease. In addition, the top pathways highlighted  
503 from IPA mirror those seen in patients with severe NAFLD (33), including cancer.

504

505 Of the most up-regulated genes in ALIOS-fed mice, two are common between males and  
506 females and both genes have key roles in driving the inflammatory phenotype. *Clec7a*  
507 encodes membrane receptors that play a role in the innate immune response. Activation of  
508 *Clec7a* leads to production of the transcription factor *NF- $\kappa$ B* (14), which induces synthesis of  
509 inflammatory cytokines such as TNF, IL-6 or IL-2 (6), suggesting that *Clec7a* is key contributor  
510 to the inflammatory profile of the liver in NAFLD. *Mmp12* is predominately expressed by  
511 macrophages and in human adipose tissue, *Mmp12* expression correlates positively with  
512 macrophage infiltration, inflammation and insulin resistance (26). *Mmp12* expression also  
513 correlates positively with arterial stiffening in mice (27), suggesting that the hepatic  
514 macrophage filtration in ALIOS-fed mice further drives progression of the disease. Among  
515 the most strongly down-regulated genes in ALIOS fed mice was *Ces2A*, encoding a hepatic  
516 serine hydrolase. In humans and mice, obesity decreases the activity of *Ces2* which leads to

517 hepatic dyslipidaemia (39). Indeed, normal expression of *Ces2* contributes to suppression of  
518 hepatic inflammation, improving adiposity and glucose tolerance (39); downregulation in the  
519 ALIOS-fed mice may therefore be a key driver of NAFLD progression. In males, three genes  
520 associated with MHC Class II were also up regulated. Previous reports have indicated disease  
521 susceptibility is strongly influenced by the MHC-II pathway; increased expression of MHC-II  
522 related genes is associated with increased hepatic fibrosis in response to toxic insults and  
523 hepatocyte damage (4, 42), suggesting the progression of NASH may be due to antigen  
524 presentation through MHC particularly in males.

525

526 Previous studies using “fast food” diets have also highlighted the characteristics of NASH (7,  
527 22). However, these diets do not contain trans-fats which Tetri *et al.*, suggested is the main  
528 driver of hepatic injury to promote fibrotic disease and its potential progression to HCCs.  
529 The use of trans-fats has recently been phased out from the food industry, due to their  
530 impact on metabolic disease. The ALIOS diet aimed to generate a rodent model which  
531 replicated the clinical characteristics of human NAFLD and NASH, and therefore trans-fats  
532 were used to drive an adverse liver phenotype rather than recapitulate current human diets.

533 Previous “fast-food” diets studies have focused primarily on the hepatic phenotype  
534 and have also detailed mitochondrial dysfunction in NASH. The ALIOS study did not include a  
535 fructose only cohort as the aim was to fully characterise a diet which induces steatosis,  
536 inflammation and fibrosis. The role of fructose in hepatic lipid accumulation has been well  
537 characterised, however recent studies using fructose only interventions have previously  
538 failed to induce hepatic steatosis and inflammation (28, 41). The combination of adverse  
539 diets and different genetic backgrounds have also made substantial contributions to pre-  
540 clinical NASH models (3, 11, 50). The ALIOS model has investigated a dietary driver of NAFLD  
541 and NASH and its plausible this may behave differently on different genetic backgrounds,  
542 but this is beyond the scope of this study. Additionally, previous pre-clinical NASH mouse

543 models have primarily neglected to analyse females and their response to these altered  
544 diets. The current ALIOS study has extended the comprehensive metabolic analysis to one  
545 year, detailed the extra-hepatic phenotype of the syndrome, as well as full transcriptomic  
546 analysis, in both male and female mice.

547

548 In conclusion, we have provided the most comprehensive, longitudinal assessment of the  
549 ALIOS diet, both with regards to its hepatic phenotype, but also its extra-hepatic  
550 manifestations. The ALIOS diet closely recapitulates many of the features of clinical NAFLD  
551 and our transcriptomic analysis has revealed many common pathways that are shared  
552 between clinical samples and the ALIOS intervention. The ALIOS model therefore represents  
553 a robust and reproducible tool to further understand the complex nature of NAFLD and its  
554 progression to the most advanced stages including NASH and HCC.

555

556 **Funding:** Medical Research Council (programme grant to J.W.T ref. MR/P011462/1; project  
557 grant to R.D.C ref: MC\_U142661184); NIHR Oxford Biomedical Research Centre (principal  
558 investigator award to J.W.T); Oxford Brookes Nigel Groome PhD Studentship (studentship  
559 award to A.A, principle investigator L.L.G).

560 **Disclosures:** No conflict(s) to disclose

561 **Acknowledgements:** The authors would like to thank the Phenotyping Team at the Mary  
562 Lyon Centre, MRC Harwell Institute for the breeding and husbandry of the mice and for  
563 conducting the phenotyping assessments. We also thank the Oxford Genomics Centre at the  
564 Wellcome Centre for Human Genetics (funded by Wellcome Trust grant reference  
565 203141/Z/16/Z) for the generation and initial processing of sequencing data.

566

567

568 **References**

569

- 570 1. **Abe N, Kato S, Tsuchida T, Sugimoto K, Saito R, Verschuren L, Kleemann R, and Oka**  
571 **K.** Longitudinal characterization of diet-induced genetic murine models of non-alcoholic  
572 steatohepatitis with metabolic, histological, and transcriptomic hallmarks of human  
573 patients. *Biology Open* 8, 2019.
- 574 2. **Armstrong MJ, Houlihan DD, Bentham L, Shaw JC, Cramb R, Olliff S, Gill PS,**  
575 **Neuberger JM, Lilford RJ, and Newsome PN.** Presence and severity of non-alcoholic fatty  
576 liver disease in a large prospective primary care cohort. *Journal of Hepatology* 56: 234-240,  
577 2012.
- 578 3. **Asgharpour A, Cazanave SC, Pacana T, Seneshaw M, Vincent R, Banini BA, Kumar**  
579 **DP, Daita K, Min HK, Mirshahi F, Bedossa P, Sun X, Hoshida Y, Koduru SV, Contaifer D,**  
580 **Warncke UO, Wijesinghe DS, and Sanyal AJ.** A diet-induced animal model of non-alcoholic  
581 fatty liver disease and hepatocellular cancer. *Journal of Hepatology* 65: 579-588, 2016.
- 582 4. **Baba Y and Doi K.** MHC class II-related genes expression in porcine-serum-induced  
583 rat hepatic fibrosis. *Experimental and Molecular Pathology* 77: 214-221, 2004.
- 584 5. **Ballestri S, Mantovani A, Nascimbeni F, Lugari S, and Lonardo A.** Extra-hepatic  
585 manifestations and complications of nonalcoholic fatty liver disease. *Future Medicinal*  
586 *Chemistry* 11: 2171-2192, 2019.
- 587 6. **Brown GD.** Dectin-1: a signalling non-TLR pattern-recognition receptor. *Nature*  
588 *Reviews Immunology* 6: 33-43, 2006.
- 589 7. **Charlton M, Krishnan A, Viker K, Sanderson S, Cazanave S, McConico A, Masuoko**  
590 **H, and Gores G.** Fast food diet mouse: novel small animal model of NASH with ballooning,  
591 progressive fibrosis, and high physiological fidelity to the human condition. *American Journal*  
592 *of Physiology* 301: G825-834, 2011.
- 593 8. **Chung GE, Kim MJ, Yim JY, Kim JS, and Yoon JW.** Sarcopenia Is Significantly  
594 Associated with Presence and Severity of Nonalcoholic Fatty Liver Disease. *Journal of Obesity*  
595 *and Metabolic Syndrome* 28: 129-138, 2019.
- 596 9. **Dowman JK, Hopkins LJ, Reynolds GM, Armstrong MJ, Nasiri M, Nikolaou N, van**  
597 **Houten EL, Visser JA, Morgan SA, Lavery GG, Oprescu A, Hübscher SG, Newsome PN, and**  
598 **Tomlinson JW.** Loss of 5 $\alpha$ -reductase type 1 accelerates the development of hepatic steatosis  
599 but protects against hepatocellular carcinoma in male mice. *Endocrinology* 154: 4536-4547,  
600 2013.
- 601 10. **Dowman JK, Hopkins LJ, Reynolds GM, Nikolaou N, Armstrong MJ, Shaw JC,**  
602 **Houlihan DD, Lalor PF, Tomlinson JW, Hübscher SG, and Newsome PN.** Development of  
603 hepatocellular carcinoma in a murine model of nonalcoholic steatohepatitis induced by use  
604 of a high-fat/fructose diet and sedentary lifestyle. *American Journal of Pathology* 184: 1550-  
605 1561, 2014.
- 606 11. **Febbraio MA, Reibe S, Shalpour S, Ooi GJ, Watt MJ, and Karin M.** Preclinical  
607 Models for Studying NASH-Driven HCC: How Useful Are They? *Cell Metabolism* 29: 18-26,  
608 2019.
- 609 12. **Font-Burgada J, Sun B, and Karin M.** Obesity and Cancer: The Oil that Feeds the  
610 Flame. *Cell Metabolism* 23: 48-62, 2016.
- 611 13. **Fraulob JC, Ogg-Diamantino R, Fernandes-Santos C, Aguila MB, and Mandarim-de-**  
612 **Lacerda CA.** A Mouse Model of Metabolic Syndrome: Insulin Resistance, Fatty Liver and Non-  
613 Alcoholic Fatty Pancreas Disease (NAFPD) in C57BL/6 Mice Fed a High Fat Diet. *Journal of*  
614 *Clinical Biochemistry and Nutrition* 46: 212-223, 2010.
- 615 14. **Gantner BN, Simmons RM, Canavera SJ, Akira S, and Underhill DM.** Collaborative  
616 induction of inflammatory responses by dectin-1 and Toll-like receptor 2. *Journal of*  
617 *Experimental Medicine* 197: 1107-1117, 2003.

- 618 15. **Ioannou GN, Green P, Lowy E, Mun EJ, and Berry K.** Differences in hepatocellular  
619 carcinoma risk, predictors and trends over time according to etiology of cirrhosis. *PLoS One*  
620 13: e0204412, 2018.
- 621 16. **Kammoun HL, Allen TL, Henstridge DC, Kraakman MJ, Peijs L, Rose-John S, and**  
622 **Febbraio MA.** Over-expressing the soluble gp130-Fc does not ameliorate methionine and  
623 choline deficient diet-induced non alcoholic steatohepatitis in mice. *PLoS One* 12: e0179099,  
624 2017.
- 625 17. **Kanwal F, Kramer JR, Mapakshi S, Natarajan Y, Chayanupatkul M, Richardson PA,**  
626 **Li L, Desiderio R, Thrift AP, Asch SM, Chu J, and El-Serag HB.** Risk of Hepatocellular Cancer  
627 in Patients With Non-Alcoholic Fatty Liver Disease. *Gastroenterology* 155: 1828-1837.e1822,  
628 2018.
- 629 18. **Kawai T, Yasuchika K, Ishii T, Miyauchi Y, Kojima H, Yamaoka R, Katayama H,**  
630 **Yoshitoshi EY, Ogiso S, Kita S, Yasuda K, Fukumitsu K, Komori J, Hatano E, Kawaguchi Y,**  
631 **and Uemoto S.** SOX9 is a novel cancer stem cell marker surrogated by osteopontin in human  
632 hepatocellular carcinoma. *Scientific Reports* 6: 30489, 2016.
- 633 19. **Kishida N, Matsuda S, Itano O, Shinoda M, Kitago M, Yagi H, Abe Y, Hibi T, Masugi**  
634 **Y, Aiura K, Sakamoto M, and Kitagawa Y.** Development of a novel mouse model of  
635 hepatocellular carcinoma with nonalcoholic steatohepatitis using a high-fat, choline-  
636 deficient diet and intraperitoneal injection of diethylnitrosamine. *BMC Gastroenterology* 16:  
637 61, 2016.
- 638 20. **Kleiner DE, Brunt EM, Van Natta M, Behling C, Contos MJ, Cummings OW, Ferrell**  
639 **LD, Liu YC, Torbenson MS, Unalp-Arida A, Yeh M, McCullough AJ, Sanyal AJ, and Network**  
640 **NSCR.** Design and validation of a histological scoring system for nonalcoholic fatty liver  
641 disease. *Hepatology* 41: 1313-1321, 2005.
- 642 21. **Koo BK, Kim D, Joo SK, Kim JH, Chang MS, Kim BG, Lee KL, and Kim W.** Sarcopenia is  
643 an independent risk factor for non-alcoholic steatohepatitis and significant fibrosis. *Journal*  
644 *of Hepatology* 66: 123-131, 2017.
- 645 22. **Krishnan A, Abdullah TS, Mounajjed T, Hartono S, McConico A, White T, LeBrasseur**  
646 **N, Lanza I, Nair S, Gores G, and Charlton M.** A longitudinal study of whole body, tissue, and  
647 cellular physiology in a mouse model of fibrosing NASH with high fidelity to the human  
648 condition. *American Journal of Physiology* 312: G666-G680, 2017.
- 649 23. **Larner DP, Morgan SA, Gathercole LL, Doig CL, Guest P, Weston C, Hazeldine J,**  
650 **Tomlinson JW, Stewart PM, and Lavery GG.** Male 11 $\beta$ -HSD1 Knockout Mice Fed Trans-Fats  
651 and Fructose Are Not Protected From Metabolic Syndrome or Nonalcoholic Fatty Liver  
652 Disease. *Endocrinology* 157: 3493-3504, 2016.
- 653 24. **Lazo M, Hernaez R, Eberhardt MS, Bonekamp S, Kamel I, Guallar E, Koteish A,**  
654 **Brancati FL, and Clark JM.** Prevalence of nonalcoholic fatty liver disease in the United States:  
655 the Third National Health and Nutrition Examination Survey, 1988-1994. *American Journal of*  
656 *Epidemiology* 178: 38-45, 2013.
- 657 25. **Le MH, Devaki P, Ha NB, Jun DW, Te HS, Cheung RC, and Nguyen MH.** Prevalence of  
658 non-alcoholic fatty liver disease and risk factors for advanced fibrosis and mortality in the  
659 United States. *PLoS One* 12: e0173499, 2017.
- 660 26. **Lee JT, Pamir N, Liu NC, Kirk EA, Averill MM, Becker L, Larson I, Hagman DK, Foster-**  
661 **Schubert KE, van Yserloo B, Bornfeldt KE, LeBoeuf RC, Kratz M, and Heinecke JW.**  
662 Macrophage metalloelastase (MMP12) regulates adipose tissue expansion, insulin  
663 sensitivity, and expression of inducible nitric oxide synthase. *Endocrinology* 155: 3409-3420,  
664 2014.
- 665 27. **Liu SL, Bae YH, Yu C, Monslow J, Hawthorne EA, Castagnino P, Branchetti E, Ferrari**  
666 **G, Damrauer SM, Puré E, and Assoian RK.** Matrix metalloproteinase-12 is an essential  
667 mediator of acute and chronic arterial stiffening. *Scientific Reports* 5: 17189, 2015.



- 668 28. **Liu XJ, Duan NN, Liu C, Niu C, Liu XP, and Wu J.** Characterization of a murine  
669 nonalcoholic steatohepatitis model induced by high fat high calorie diet plus fructose and  
670 glucose in drinking water. *Laboratory Investigation* 98: 1184-1199, 2018.
- 671 29. **Lo L, McLennan SV, Williams PF, Bonner J, Chowdhury S, McCaughan GW, Gorrell**  
672 **MD, Yue DK, and Twigg SM.** Diabetes is a progression factor for hepatic fibrosis in a high fat  
673 fed mouse obesity model of non-alcoholic steatohepatitis. *Journal of Hepatology* 55: 435-  
674 444, 2011.
- 675 30. **Love MI, Anders S, Kim V, and Huber W.** RNA-Seq workflow: gene-level exploratory  
676 analysis and differential expression. *F1000Res* 4: 1070, 2015.
- 677 31. **Lunter G and Goodson M.** Stampy: a statistical algorithm for sensitive and fast  
678 mapping of Illumina sequence reads. *Genome Research* 21: 936-939, 2011.
- 679 32. **Mantovani A, Turino T, Lando MG, Gjini K, Byrne CD, Zusi C, Ravaioli F, Colecchia A,**  
680 **Maffei C, Salvagno G, Lippi G, Bonora E, and Targher G.** Screening for non-alcoholic fatty  
681 liver disease using liver stiffness measurement and its association with chronic kidney  
682 disease and cardiovascular complications in patients with type 2 diabetes. *Diabetes &*  
683 *Metabolism*, 2019.
- 684 33. **Moylan CA, Pang H, Dellinger A, Suzuki A, Garrett ME, Guy CD, Murphy SK, Ashley-**  
685 **Koch AE, Choi SS, Michelotti GA, Hampton DD, Chen Y, Tillmann HL, Hauser MA,**  
686 **Abdelmalek MF, and Diehl AM.** Hepatic gene expression profiles differentiate  
687 presymptomatic patients with mild versus severe nonalcoholic fatty liver disease.  
688 *Hepatology* 59: 471-482, 2014.
- 689 34. **Nakagawa H, Umemura A, Taniguchi K, Font-Burgada J, Dhar D, Ogata H, Zhong Z,**  
690 **Valasek MA, Seki E, Hidalgo J, Koike K, Kaufman RJ, and Karin M.** ER stress cooperates with  
691 hypernutrition to trigger TNF-dependent spontaneous HCC development. *Cancer Cell* 26:  
692 331-343, 2014.
- 693 35. **Natri HM, Wilson MA, and Buetow KH.** Distinct molecular etiologies of male and  
694 female hepatocellular carcinoma. *BMC Cancer* 19: 951, 2019.
- 695 36. **Park EJ, Lee JH, Yu GY, He G, Ali SR, Holzer RG, Osterreicher CH, Takahashi H, and**  
696 **Karin M.** Dietary and genetic obesity promote liver inflammation and tumorigenesis by  
697 enhancing IL-6 and TNF expression. *Cell* 140: 197-208, 2010.
- 698 37. **Park YN.** Update on precursor and early lesions of hepatocellular carcinomas.  
699 *Archives of Pathology and Laboratory Medicine* 135: 704-715, 2011.
- 700 38. **Paterson JM, Morton NM, Fievet C, Kenyon CJ, Holmes MC, Staels B, Seckl JR, and**  
701 **Mullins JJ.** Metabolic syndrome without obesity: Hepatic overexpression of 11beta-  
702 hydroxysteroid dehydrogenase type 1 in transgenic mice. *PNAS* 101: 7088-7093, 2004.
- 703 39. **Ruby MA, Massart J, Hunerdosse DM, Schönke M, Correia JC, Louie SM, Ruas JL,**  
704 **Näslund E, Nomura DK, and Zierath JR.** Human Carboxylesterase 2 Reverses Obesity-  
705 Induced Diacylglycerol Accumulation and Glucose Intolerance. *Cell Reports* 18: 636-646,  
706 2017.
- 707 40. **Salleng KJ, Revetta FL, Deane NG, and Washington MK.** The Applicability of a  
708 Human Immunohistochemical Panel to Mouse Models of Hepatocellular Neoplasia.  
709 *Comparative Medicine* 65: 398-408, 2015.
- 710 41. **Savari F, Mard SA, Badavi M, Rezaie A, and Gharib-Naseri MK.** A new method to  
711 induce nonalcoholic steatohepatitis (NASH) in mice. *BMC Gastroenterology* 19: 125, 2019.
- 712 42. **Singer JB, Lewitzky S, Leroy E, Yang F, Zhao X, Klickstein L, Wright TM, Meyer J, and**  
713 **Paulding CA.** A genome-wide study identifies HLA alleles associated with lumiracoxib-related  
714 liver injury. *Nature Genetics* 42: 711-714, 2010.
- 715 43. **Softic S, Cohen DE, and Kahn CR.** Role of Dietary Fructose and Hepatic De Novo  
716 Lipogenesis in Fatty Liver Disease. *Digestive Diseases and Science* 61: 1282-1293, 2016.
- 717 44. **Sun DQ, Ye FZ, Kani HT, Yang JR, Zheng KI, Zhang HY, Targher G, Byrne CD, Chen**  
718 **YP, Yuan WJ, Yilmaz Y, and Zheng MH.** Higher liver stiffness scores are associated with early

- 719 kidney dysfunction in patients with histologically proven non-cirrhotic NAFLD. *Diabetes &*  
720 *Metabolism*, 2019.
- 721 45. **Tandra S, Yeh MM, Brunt EM, Vuppalanchi R, Cummings OW, Ünalp-Arida A,**  
722 **Wilson LA, and Chalasani N.** Presence and significance of microvesicular steatosis in  
723 nonalcoholic fatty liver disease. *Journal of Hepatology* 55: 654-659, 2011.
- 724 46. **Tetri LH, Basaranoglu M, Brunt EM, Yerian LM, and Neuschwander-Tetri BA.** Severe  
725 NAFLD with hepatic necroinflammatory changes in mice fed trans fats and a high-fructose  
726 corn syrup equivalent. *American Journal of Physiology* 295: G987-995, 2008.
- 727 47. **Tsuchida T, Lee YA, Fujiwara N, Ybanez M, Allen B, Martins S, Fiel MI, Goossens N,**  
728 **Chou HI, Hoshida Y, and Friedman SL.** A simple diet- and chemical-induced murine NASH  
729 model with rapid progression of steatohepatitis, fibrosis and liver cancer. *Journal of*  
730 *Hepatology* 69: 385-395, 2018.
- 731 48. **VanWagner LB and Rinella ME.** Extrahepatic Manifestations of Nonalcoholic Fatty  
732 Liver Disease. *Current Hepatology Reports* 15: 75-85, 2016.
- 733 49. **Weber A, Boger R, Vick B, Urbanik T, Haybaeck J, Zoller S, Teufel A, Krammer PH,**  
734 **Opferman JT, Galle PR, Schuchmann M, Heikenwalder M, and Schulze-Bergkamen H.**  
735 Hepatocyte-specific deletion of the antiapoptotic protein myeloid cell leukemia-1 triggers  
736 proliferation and hepatocarcinogenesis in mice. *Hepatology* 51: 1226-1236, 2010.
- 737 50. **Wei G, An P, Vaid KA, Nasser I, Huang P, Tan L, Zhao S, Schuppan D, and Popov YV.**  
738 Comparison of murine steatohepatitis models identifies a dietary intervention with robust  
739 fibrosis, ductular reaction, and rapid progression to cirrhosis and cancer. *American Journal of*  
740 *Physiology* 318: G174-G188, 2020.
- 741 51. **Yang JD, Ahmed F, Mara KC, Addissie BD, Allen AM, Gores GJ, and Roberts LR.**  
742 Diabetes Is Associated With Increased Risk of Hepatocellular Carcinoma in Patients With  
743 Cirrhosis From Nonalcoholic Fatty Liver Disease. *Hepatology*: doi: 10.1002/hep.30858, 2019.
- 744 52. **Zhang X.** NAFLD Related-HCC: The Relationship with Metabolic Disorders. *Advances*  
745 *in Experimental Medicine and Biology* 1061: 55-62, 2018.

747

748

749

750

751 **Fig.1.** The ALIOS diet increased bodyweight and fat mass in male and female mice from 11-  
752 to 52-weeks. (A) Body weight curves for male (NC n=29, ALIOS n=27) and (B) female NC  
753 (n=30) and ALIOS (n=30) fed mice and DXA determined lean and fat mass in (C) male (NC  
754 n=17, ALIOS n=12) and (D) female (NC n=15, ALIOS n=15) mice from 15- to 52-weeks.  
755 Changes in adipose depot mass in male (E) and (F) female NC and ALIOS fed mice at 26- and  
756 52-weeks. GF=gonadal fat, Mes=mesenteric fat, PR=perirenal fat, BAT=brown adipose tissue.  
757 Data expressed as mean  $\pm$  SEM. 26-weeks: NC males n=12, ALIOS males n=15, NC females  
758 n=15, ALIOS females n=15. 52-weeks: NC males n=17, ALIOS males n=12, NC females n=15,

759 ALIOS females n=15. \* $P$ <0.05, \*\* $P$ <0.01, \*\*\* $P$ <0.001 significantly different from mice fed NC  
760 at each time point.

761

762

763 **Fig.2.** ALIOS fed mice have normal glucose tolerance. ipGTTs in NC and ALIOS fed male (A)  
764 and female (B) mice at 15-, 25-, 37- and 49-weeks. ipGTT represented as AUCs in (C) male  
765 and (D) female NC and ALIOS fed mice at 15-, 25-, 37- and 49-weeks. AUCs of serum insulin  
766 collected at t=0, 60 and 120 minutes during the ipGTT in (E) male and (F) female mice.  
767 ipGTT: i.p. glucose tolerance test, AUC; area under the curve. Data expressed as mean  $\pm$   
768 SEM. n=7 in each group at each time point, \* $P$ <0.05, \*\* $P$ <0.01.

769

770 **Fig.3.** Male and female ALIOS fed mice are insulin resistant. ipITT represented as AUCs in (A)  
771 male and (B) female NC and ALIOS fed mice at 25-, 37- and 50-weeks. ipITT: i.p. insulin  
772 tolerance test. HOMA-IR of (C) male and (D) female ALIOS and NC fed mice at 15-, 25-, 37-  
773 and 49-weeks. Data expressed as mean  $\pm$  SEM. n=7 in each group at each time point,  
774 \* $P$ <0.05, \*\* $P$ <0.01, \*\*\* $P$ <0.001.

775

776 **Fig.4.** ALIOS drives hepatic steatosis. Liver mass of (A) male and (B) female and hepatic TAG  
777 content in (C) male and (D) female NC and ALIOS fed mice at 26- and 52-weeks (26-weeks:  
778 NC males n=12, ALIOS males n=15, NC females n=15, ALIOS females n=15. 52-weeks: NC  
779 males n=17, ALIOS males n=12, NC females n=15, ALIOS females n=15). Representative H&E  
780 images from male mice at 52-weeks fed NC (E) and ALIOS (F) depicting macro- and micro-  
781 vesicular lipid droplets. Data expressed as mean  $\pm$  SEM. Scale bar is 25 $\mu$ m. ALIOS fed male  
782 and female mice had altered expression of genes associated with lipid metabolism (G:  
783 males, H: females) insulin signalling (I: males, J: females). n=8 in each group. Genes are

784 expressed as fold changes in  $\log_{10}$  compared to NC. \* $P$ <0.05, \*\* $P$ <0.01, \*\*\* $P$ <0.001,  
785 \*\*\*\* $P$ <0.0001.

786

787 **Fig.5.** Mice fed ALIOS have increased hepatic inflammation. Histologically determined  
788 inflammation score of (A) male and (B) female NC and ALIOS fed mice at 26- (NC males  
789  $n$ =12, ALIOS males  $n$ =15, NC females  $n$ =15, ALIOS females  $n$ =15) and 52-weeks (NC males  
790  $n$ =17, ALIOS males  $n$ =12, NC females  $n$ =15, ALIOS females  $n$ =15). Data expressed as mean  $\pm$   
791 SEM. Both male (C) and female (D) mice had increased hepatic expression of genes involved  
792 in inflammation, including macrophage infiltration compared to NC fed mice at 52-weeks.  
793  $n$ =8 in each group. \* $P$ <0.05, \*\* $P$ <0.01, \*\*\* $P$ <0.001, \*\*\*\* $P$ <0.0001

794

795 **Fig.6.** ALIOS drives hepatic fibrosis in aged mice. Percentage fibrosis determined by Sirius red  
796 staining in male (A) and female (B) NC and ALIOS fed mice at 26- (NC males  $n$ =12, ALIOS  
797 males  $n$ =15, NC females  $n$ =15, ALIOS females  $n$ =15) and 52-weeks (NC males  $n$ =17, ALIOS  
798 males  $n$ =12, NC females  $n$ =15, ALIOS females  $n$ =15) and hepatic expression of genes  
799 associated with cell adhesion in male (C) and female (D) ALIOS fed mice ( $n$ =8 in each group,  
800 genes are expressed as fold changes in  $\log_{10}$  compared to NC). (E) Western blotting of Col1a1  
801 in male and female (F) NC and ALIOS fed mice at 52-weeks ( $n$ =10 in each group). Data  
802 expressed as mean  $\pm$  SEM, \* $P$ <0.05, \*\* $P$ <0.01, \*\*\* $P$ <0.001, \*\*\*\* $P$ <0.0001. Representative  
803 images depicting Sirius red staining in male NC (G) and ALIOS (H) mice at 52-weeks. (I) H&E  
804 staining of a potential HCC from a male ALIOS fed mouse at 52-weeks highlighting (J) the  
805 compressed border of cells (\*) and multinucleic cells (arrow). An example of positive Sox9  
806 (K) and glutamine synthetase (L) labelling in a HCC from an ALIOS fed male mouse at 52-  
807 weeks.

808

809 **Fig.7.** Hierarchical clustering analysis of the top 100 DEGs from male (A) and (B) female NC  
810 and ALIOS fed mice at 52-weeks. Data presented in a heat-map format in which NC and  
811 ALIOS separated into columns and genes in rows. Red corresponds to genes which are  
812 upregulated in ALIOS compared to NC and blue corresponds to those that are  
813 downregulated. Enriched gene pathways of ALIOS fed mice. (C) Upregulated and (D)  
814 downregulated gene ontology pathways in male mice; (E) upregulated and (F) down  
815 regulated pathways in females. Pathways ranked by p-values.

816

817 **Fig.8.** (A) ALIOS fed male mice and human patients with NASH share 22.5% of DEGs. (B)  
818 Hierarchical clustering analysis of the top 30 DEGs from human NASH and ALIOS fed male  
819 mice. (C) Overlapping DEGs are associated with metabolism, inflammation and cell adhesion  
820 (genes are expressed as fold changes in  $\log_{10}$  compared to NC) and (D) gene ontology of the  
821 top 100 overlapping DEGs are associated with alterations in metabolic pathways, immune  
822 response and cell adhesion. Pathways ranked by p-values.

823

**Table 1.** Mean  $\pm$  SEM circulating serum levels of lipids

Males (mmol/l)	16w		25w		37w		52w	
	NC	ALIOS	NC	ALIOS	NC	ALIOS	NC	ALIOS
Total cholesterol	2.6 $\pm$ 0.1	3.9 $\pm$ 0.2***	2.1 $\pm$ 0.1	4.1 $\pm$ 0.2****	2.4 $\pm$ 0.1	4.6 $\pm$ 0.3****	2.5 $\pm$ 0.2	5.8 $\pm$ 0.4****
HDL	1.8 $\pm$ 0.1	2.7 $\pm$ 0.1****	1.5 $\pm$ 0.1	2.9 $\pm$ 0.1****	1.7 $\pm$ 0.1	3.1 $\pm$ 0.2****	1.7 $\pm$ 0.1	3.7 $\pm$ 0.4****
LDL	0.59 $\pm$ 0.02	0.9 $\pm$ 0.1***	0.43 $\pm$ 0.03	0.9 $\pm$ 0.1****	0.6 $\pm$ 0.1	1.3 $\pm$ 0.2****	0.5 $\pm$ 0.1	1.8 $\pm$ 0.2****
TAG	1.1 $\pm$ 0.1	1.2 $\pm$ 0.1	1.0 $\pm$ 0.1	1.0 $\pm$ 0.1	1.3 $\pm$ 0.1	1.1 $\pm$ 0.1	0.94 $\pm$ 0.04	0.67 $\pm$ 0.04****
Free fatty acids	1.7 $\pm$ 0.1	1.5 $\pm$ 0.1	0.9 $\pm$ 0.1	0.81 $\pm$ 0.05	1.9 $\pm$ 0.1	1.8 $\pm$ 0.1	0.8 $\pm$ 0.1	0.67 $\pm$ 0.04*
<b>Females (mmol/l)</b>								
Total cholesterol	2.0 $\pm$ 0.1	2.4 $\pm$ 0.2*	2.0 $\pm$ 0.1	2.8 $\pm$ 0.2***	1.7 $\pm$ 0.1	2.9 $\pm$ 0.2***	1.7 $\pm$ 0.1	3.2 $\pm$ 0.4****
HDL	1.3 $\pm$ 0.1	1.5 $\pm$ 0.1	1.4 $\pm$ 0.1	2.0 $\pm$ 0.1***	1.2 $\pm$ 0.1	2.1 $\pm$ 0.1***	1.2 $\pm$ 0.1	2.1 $\pm$ 0.2****
LDL	0.48 $\pm$ 0.03	0.57 $\pm$ 0.04	0.45 $\pm$ 0.02	0.61 $\pm$ 0.04****	0.43 $\pm$ 0.01	0.71 $\pm$ 0.08**	0.36 $\pm$ 0.02	0.74 $\pm$ 0.13****
TAG	0.8 $\pm$ 0.1	1.0 $\pm$ 0.1	0.65 $\pm$ 0.03	0.55 $\pm$ 0.02*	0.97 $\pm$ 0.02	0.71 $\pm$ 0.04****	0.81 $\pm$ 0.03	0.55 $\pm$ 0.03**
Free fatty acids	1.7 $\pm$ 0.1	1.7 $\pm$ 0.1	0.81 $\pm$ 0.04	0.64 $\pm$ 0.04**	1.95 $\pm$ 0.15	1.37 $\pm$ 0.07****	0.97 $\pm$ 0.06	0.69 $\pm$ 0.04**

\* Significantly different from NC at same age P<0.05, \*\* P<0.01, \*\*\* P<0.001, \*\*\*\*P<0.0001. n=12-15 in each group.

**Table 2.** Mean  $\pm$  SEM circulating serum levels of renal and liver biochemistry

Males	16w		25w		37w		52w	
	NC	ALIOS	NC	ALIOS	NC	ALIOS	NC	ALIOS
Creatinine (mg/dl)	N/A		0.69 $\pm$ 0.06	0.81 $\pm$ 0.11	N/A		0.67 $\pm$ 0.08	0.96 $\pm$ 0.08*
ALP (U/l)	76.6 $\pm$ 3.3	72.6 $\pm$ 4.0	64.9 $\pm$ 2.0	75.2 $\pm$ 7.6	70.1 $\pm$ 2.9	88.7 $\pm$ 12.1	66.2 $\pm$ 3.1	118.5 $\pm$ 11.0****
ALT (U/l)	42.1 $\pm$ 1.9	83.7 $\pm$ 23.9	33.0 $\pm$ 2.6	99.9 $\pm$ 16.4**	34.4 $\pm$ 2.9	238.0 $\pm$ 82.4**	38.0 $\pm$ 4.0	291.2 $\pm$ 47.4****
AST (U/l)	93.7 $\pm$ 6.3	126.3 $\pm$ 22.1	69.5 $\pm$ 8.1	135.9 $\pm$ 17.0**	72.4 $\pm$ 7.9	250.7 $\pm$ 80.5*	72.4 $\pm$ 4.6	346.3 $\pm$ 50.8****
AST/ALT ratio	2.2 $\pm$ 0.1	1.7 $\pm$ 0.1*	2.2 $\pm$ 0.3	1.6 $\pm$ 0.2	2.2 $\pm$ 0.3	1.1 $\pm$ 0.1**	2.0 $\pm$ 0.1	1.2 $\pm$ 0.1****
Total bilirubin ( $\mu$ mol/l)	3.7 $\pm$ 0.5	2.9 $\pm$ 0.4	1.9 $\pm$ 0.1	1.8 $\pm$ 0.1	2.2 $\pm$ 0.2	2.1 $\pm$ 0.1	1.9 $\pm$ 0.1	1.9 $\pm$ 0.1
<b>Females</b>								
Creatinine (mg/dl)	N/A		0.62 $\pm$ 0.07	0.65 $\pm$ 0.08	N/A		0.64 $\pm$ 0.07	0.91 $\pm$ 0.08
ALP (U/l)	138.9 $\pm$ 11.3	120.9 $\pm$ 8.1	105.1 $\pm$ 3.6	108.4 $\pm$ 4.4	122.7 $\pm$ 15.1	142.3 $\pm$ 9.8	130.5 $\pm$ 7.5	138.5 $\pm$ 13.7
ALT (U/l)	43.9 $\pm$ 7.2	46.7 $\pm$ 6.8	28.5 $\pm$ 1.4	136.3 $\pm$ 32.8***	33.0 $\pm$ 1.7	226.3 $\pm$ 54.4***	37.7 $\pm$ 4.1	310.4 $\pm$ 41.5***
AST (U/l)	114.9 $\pm$ 20.5	125.9 $\pm$ 11.0	68.3 $\pm$ 3.6	251.7 $\pm$ 47.0***	83.7 $\pm$ 6.4	338.5 $\pm$ 55.4***	101.3 $\pm$ 8.6	501.3 $\pm$ 45.3***
AST/ALT ratio	2.6 $\pm$ 0.1	2.8 $\pm$ 0.2	2.4 $\pm$ 0.1	2.2 $\pm$ 0.2	2.5 $\pm$ 0.1	1.7 $\pm$ 0.1***	2.8 $\pm$ 0.2	1.7 $\pm$ 0.1***
Total bilirubin ( $\mu$ mol/l)	3.2 $\pm$ 0.6	4.4 $\pm$ 0.4	1.7 $\pm$ 0.1	1.9 $\pm$ 0.1	2.3 $\pm$ 0.2	2.1 $\pm$ 0.2	1.7 $\pm$ 0.1	2.0 $\pm$ 0.1*

\* Significantly different from NC at same age P<0.05, \*\*P<0.01, \*\*\* P<0.001,\*\*\*\* P<0.0001. N/A Serum not analysed at this time point. n= 12-15 in each group. Creatinine n=10 in each group.

**Table 3.** The 10 most up- and down-regulated genes in NC vs ALIOS liver tissue at 52-weeks

Gene	Description	Log Fold	FDR
<b>Males</b>			
<i>Clec7a</i>	C-type lectin domain family 7	2.3128	7.98x10 <sup>-33</sup>
<i>Mmp12</i>	matrix metalloproteinase 12	4.1723	7.04x10 <sup>-31</sup>
<i>H2-Ab1</i>	histocompatibility 2, class II antigen A, beta 1	1.9017	4.10x10 <sup>-29</sup>
<i>Cx3cr1</i>	chemokine (C-X3-C motif) receptor 1	2.8669	1.24x10 <sup>-28</sup>
<i>H2-Aa</i>	histocompatibility 2, class II antigen A, alpha	2.1164	2.10x10 <sup>-28</sup>
<i>Tmem86a</i>	transmembrane protein 86A	1.7757	4.03x10 <sup>-28</sup>
<i>Col1a1</i>	collagen, type I, alpha 1	3.5204	1.72x10 <sup>-26</sup>
<i>Ephb2</i>	Eph receptor B2	4.7443	2.27x10 <sup>-25</sup>
<i>Cd63</i>	CD63 antigen	3.0092	3.45x10 <sup>-25</sup>
<i>H2-Eb1</i>	histocompatibility 2, class II antigen E beta	1.9343	1.11x10 <sup>-24</sup>
<i>Ces2a</i>	carboxylesterase 2A	-1.9190	7.04x10 <sup>-31</sup>
<i>Ces1b</i>	carboxylesterase 1B	-1.3651	6.89x10 <sup>-23</sup>
<i>Tnfaip8l1</i>	tumour necrosis factor, alpha-induced protein 8-like 1	-1.0119	1.99x10 <sup>-17</sup>
<i>Scarb2</i>	scavenger receptor class B, member 2	-0.7034	3.34x10 <sup>-14</sup>
<i>Retsat</i>	retinol saturase (all trans retinol 13,14 reductase)	-1.0527	6.13x10 <sup>-14</sup>
<i>Marf1</i>	meiosis regulator and mRNA stability 1	-0.7292	2.89x10 <sup>-13</sup>
<i>Tuba4a</i>	tubulin, alpha 4A	-0.9631	3.80x10 <sup>-13</sup>
<i>Hectd1</i>	HECT domain E3 ubiquitin protein ligase 1	-0.6121	9.50x10 <sup>-13</sup>
<i>Angptl4</i>	angiopoietin-like 4	-1.0041	1.27x10 <sup>-12</sup>
<i>Pxmp4</i>	peroxisomal membrane protein 4	-0.9919	1.46x10 <sup>-12</sup>
<b>Females</b>			
<i>Wfdc2</i>	WAP four-disulfide core domain 2	2.6371	1.97x10 <sup>-40</sup>
<i>Uap1l1</i>	UDP-N-acetylglucosamine pyrophosphorylase 1-like 1	2.6742	6.04x10 <sup>-39</sup>
<i>Ifi2712b</i>	interferon, alpha-inducible protein 27 like 2B	2.8447	2.95x10 <sup>-37</sup>
<i>Ly6d</i>	lymphocyte antigen 6 complex, locus D	3.6763	7.04x10 <sup>-29</sup>
<i>Clec7a</i>	C-type lectin domain family 7, member a	2.4672	4.90x10 <sup>-28</sup>
<i>Mmp12</i>	matrix metalloproteinase 12	5.0590	5.69x10 <sup>-28</sup>
<i>Ms4a6d</i>	membrane-spanning 4-domains, subfamily A, member 6D	2.0780	7.87x10 <sup>-28</sup>
<i>Hcar2</i>	hydroxycarboxylic acid receptor 2	2.5398	1.12x10 <sup>-27</sup>
<i>Lpl</i>	lipoprotein lipase	2.5220	1.16x10 <sup>-27</sup>
<i>Osbpl3</i>	oxysterol binding protein-like 3	3.5456	2.10x10 <sup>-27</sup>
<i>Abhd6</i>	abhydrolase domain containing 6	-1.1633	6.92x10 <sup>-27</sup>
<i>Gm3787</i>	Predicted gene 3787*	-2.6100	1.97x10 <sup>-22</sup>
<i>Ces2a</i>	carboxylesterase 2A	-1.4585	6.56x10 <sup>-19</sup>
<i>Mttp</i>	microsomal triglyceride transfer protein	-0.8436	2.59x10 <sup>-17</sup>
<i>Cyp2c23</i>	cytochrome P450, family 2, subfamily c, polypeptide 23	-1.6328	1.10x10 <sup>-16</sup>
<i>Avpr1a</i>	arginine vasopressin receptor 1A	-1.5448	2.88x10 <sup>-16</sup>
<i>Fam234b</i>	family with sequence similarity 234, member B	-1.2050	9.72x10 <sup>-16</sup>
<i>Sult5a1</i>	sulfotransferase family 5A, member 1	-2.6802	1.79x10 <sup>-15</sup>
<i>Cyp4a10</i>	cytochrome P450, family 4, subfamily a, polypeptide 10	-1.2606	2.61x10 <sup>-14</sup>
<i>Sult3a2</i>	sulfotransferase family 3A, member 2	-3.7032	9.57x10 <sup>-14</sup>

\*function of predicted genes unknown in current annotation

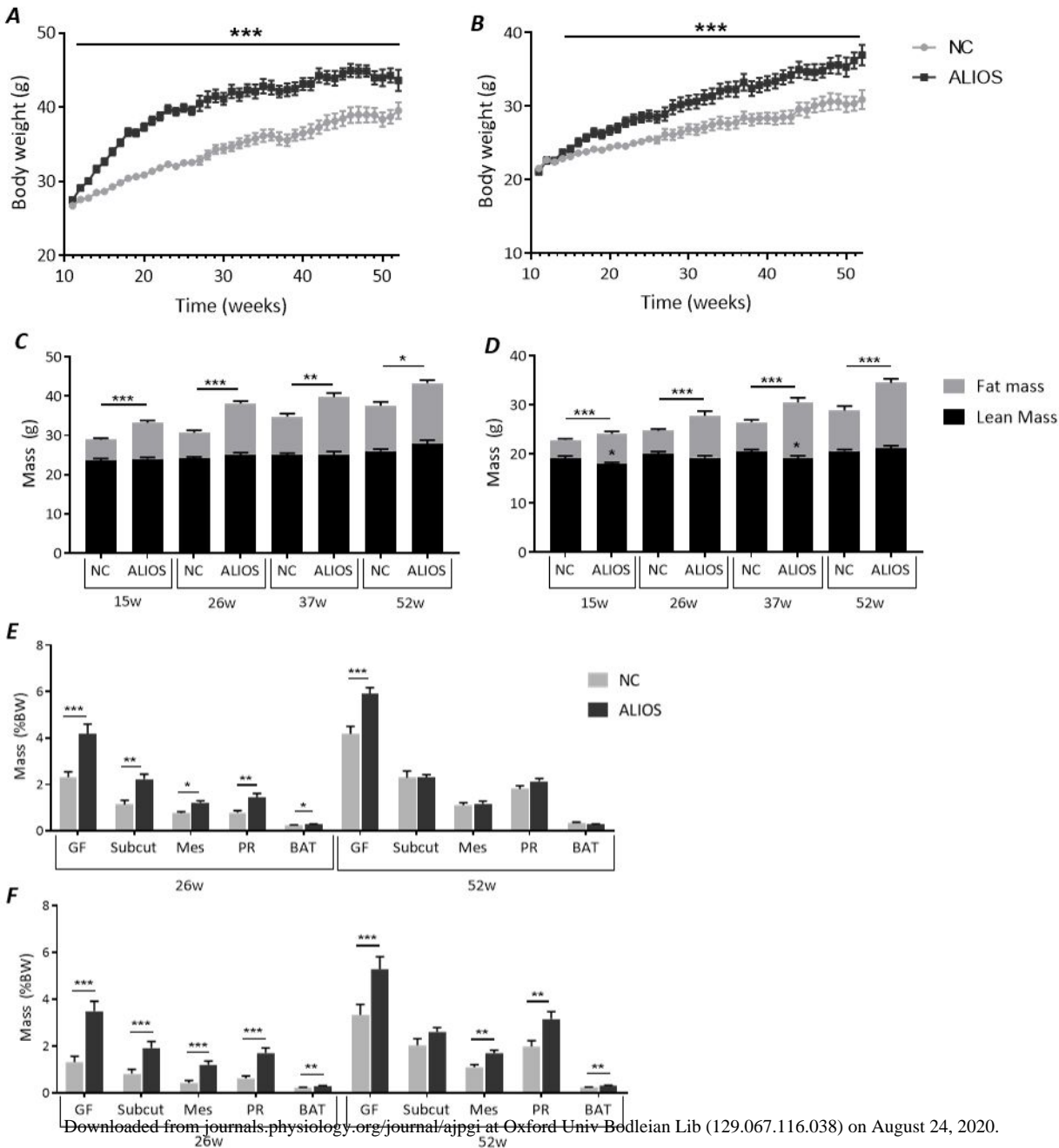


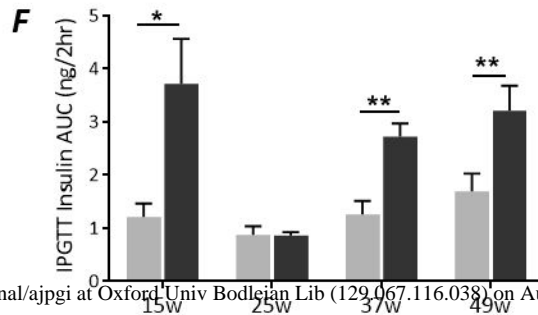
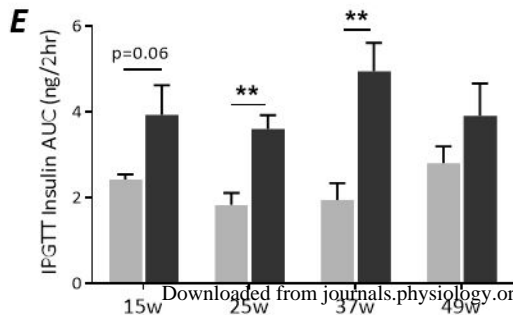
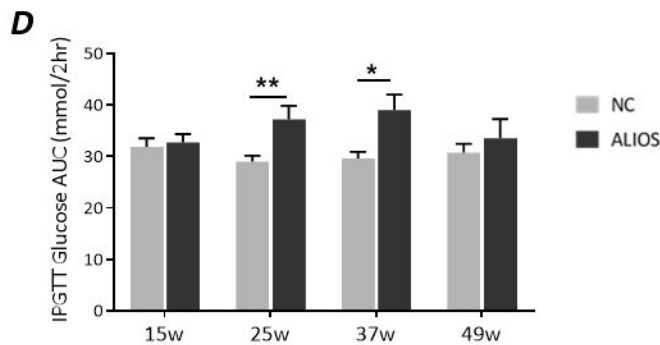
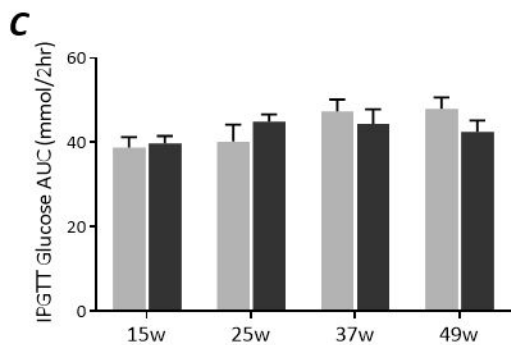
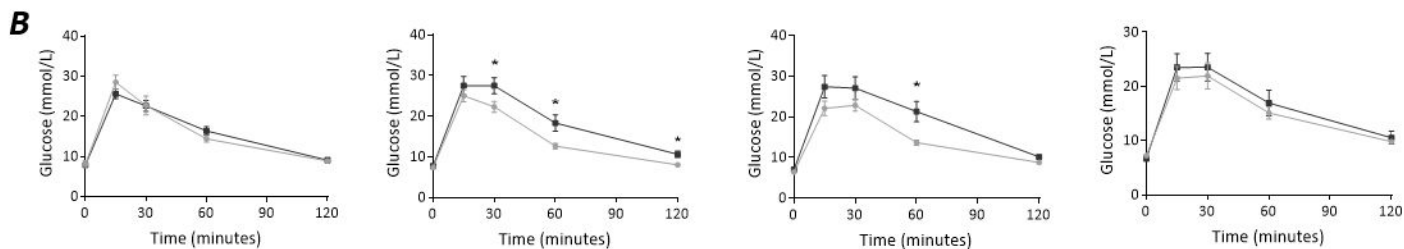
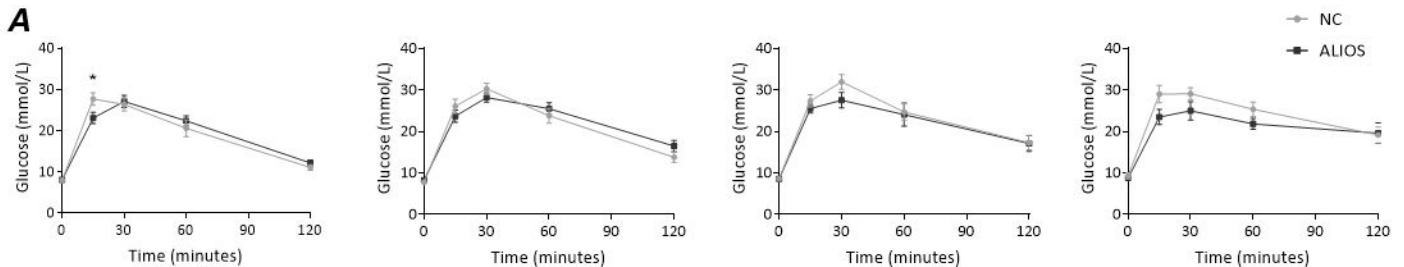


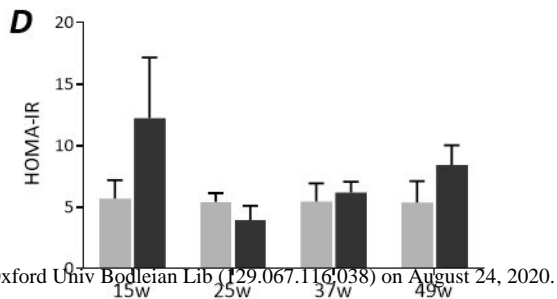
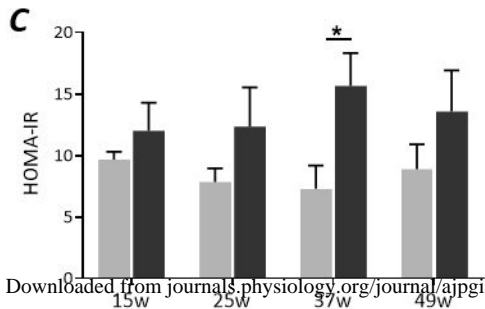
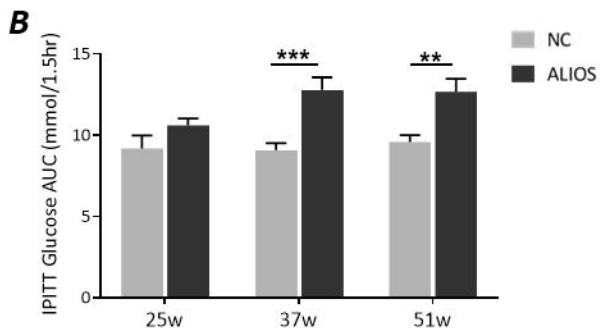
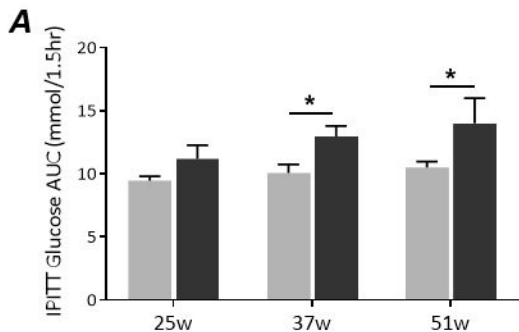
**Table 4.** IPA of differentiated genes in male and female ALIOS fed mice at 52-weeks

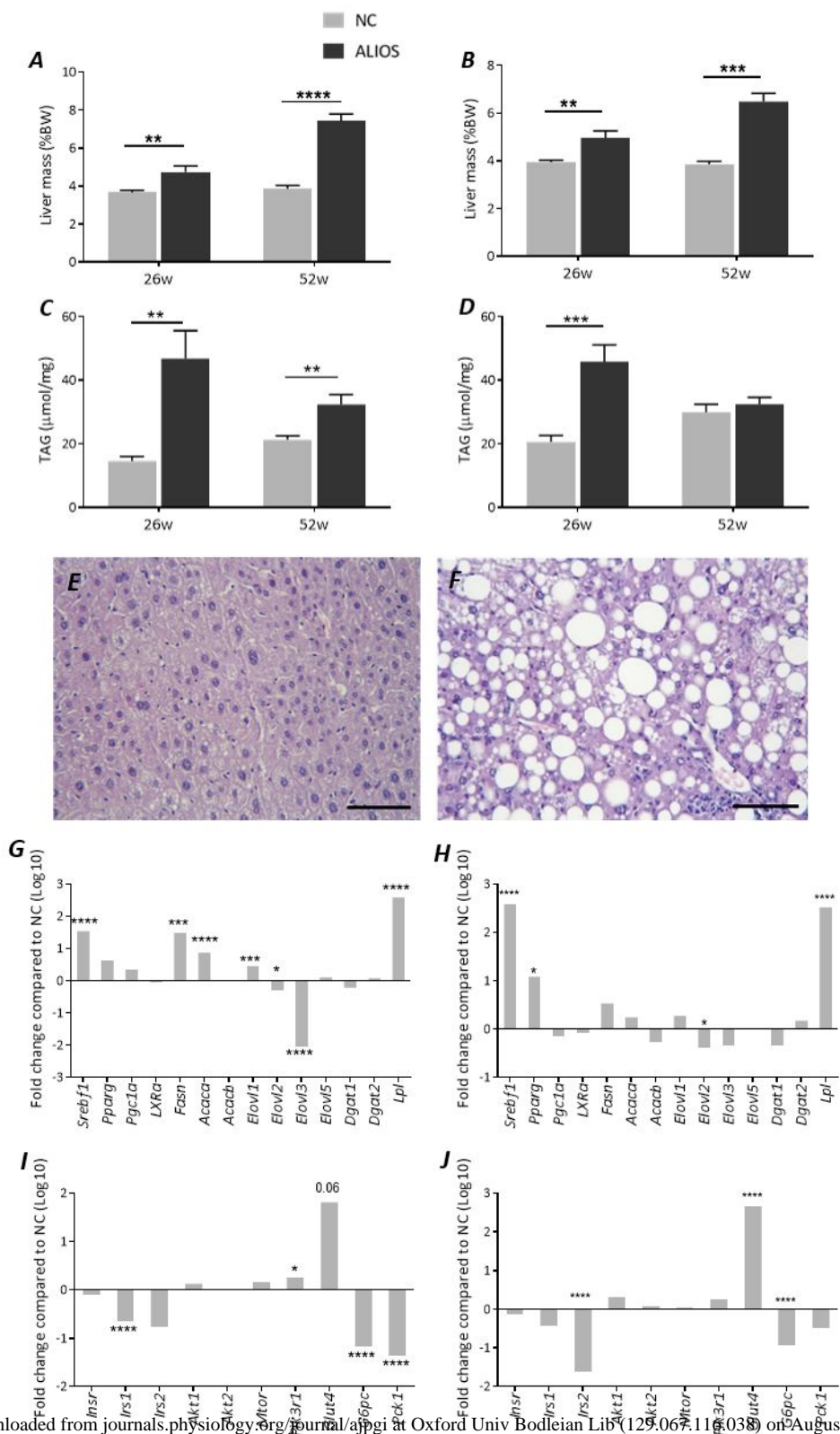
Biological Function	P-value	Genes (n)
<b>Males</b>		
<b>Diseases and Disorders</b>		
Cancer	$1.04 \times 10^{-14} - 1.69 \times 10^{-88}$	4093
Organismal Injury and Abnormalities	$1.04 \times 10^{-14} - 1.69 \times 10^{-88}$	4206
Endocrine System Disorders	$1.03 \times 10^{-27} - 2.92 \times 10^{-70}$	3316
Gastrointestinal Disease	$6.12 \times 10^{-15} - 9.14 \times 10^{-57}$	3682
Inflammatory Response	$9.02 \times 10^{-15} - 7.51 \times 10^{-54}$	1364
<b>Molecular and Cellular Functions</b>		
Cell Death and Survival	$7.61 \times 10^{-15} - 2.49 \times 10^{-72}$	1622
Cellular Movement	$7.21 \times 10^{-15} - 6.10 \times 10^{-68}$	1216
Cellular Compromise	$5.16 \times 10^{-19} - 7.51 \times 10^{-54}$	354
Cell-To-Cell Signalling and Interaction	$1.07 \times 10^{-14} - 6.98 \times 10^{-41}$	953
Lipid Metabolism	$1.10 \times 10^{-14} - 1.40 \times 10^{-39}$	797
<b>Top Toxicology list</b>		<b>Overlap (ratio)</b>
NRF2-mediated Oxidative Stress Response	$2.83 \times 10^{-15}$	42.1% (101/240)
Liver Necrosis/Cell Death	$6.98 \times 10^{-15}$	38.5% (124/322)
Renal Necrosis/Cell Death	$1.40 \times 10^{-14}$	33.3% (191/573)
Hepatic Fibrosis	$1.41 \times 10^{-13}$	51.4% (57/111)
Xenobiotic Metabolism Signalling	$1.19 \times 10^{-11}$	35.2% (123/349)
<b>Females</b>		
<b>Diseases and Disorders</b>		
Cancer	$8.17 \times 10^{-15} - 2.35 \times 10^{-78}$	3434
Organismal Injury and Abnormalities	$1.86 \times 10^{-14} - 2.35 \times 10^{-78}$	3528
Endocrine System Disorders	$1.94 \times 10^{-36} - 3.14 \times 10^{-64}$	2815
Inflammatory Response	$1.29 \times 10^{-14} - 7.07 \times 10^{-56}$	1187
Gastrointestinal Disease	$1.09 \times 10^{-14} - 3.97 \times 10^{-51}$	3122
<b>Molecular and Cellular Functions</b>		
Cell Death and Survival	$1.35 \times 10^{-14} - 7.31 \times 10^{-58}$	1375
Cellular Movement	$1.32 \times 10^{-14} - 2.23 \times 10^{-55}$	999
Cellular Compromise	$1.35 \times 10^{-14} - 4.09 \times 10^{-55}$	374
Cellular Function and Maintenance	$2.32 \times 10^{-15} - 1.81 \times 10^{-50}$	1237
Cell-To-Cell Signalling and Interaction	$1.75 \times 10^{-14} - 1.79 \times 10^{-41}$	707
<b>Top Toxicology list</b>		<b>Overlap (ratio)</b>
Hepatic Fibrosis	$2.00 \times 10^{-16}$	50.5% (56/111)
Renal Necrosis/Cell Death	$5.35 \times 10^{-13}$	28.4% (163/573)
Liver Necrosis/Cell Death	$1.11 \times 10^{-12}$	32.6% (105/322)
Increases Liver Steatosis	$3.83 \times 10^{-12}$	45.0% (49/109)
LXR/RXR Activation	$5.63 \times 10^{-11}$	41.5% (51/123)

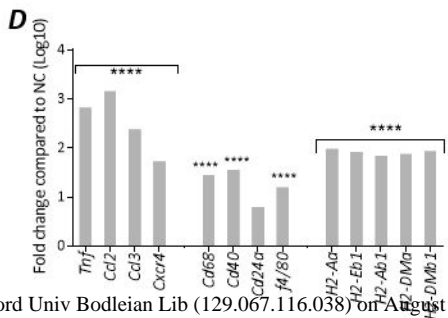
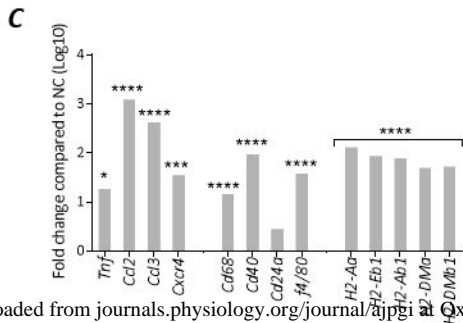
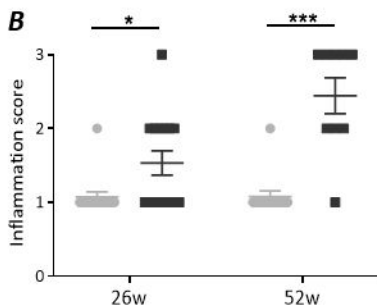
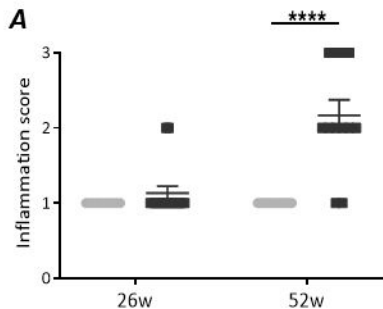
Data represent the number of genes up- or down-regulated in ALIOS fed mice at 52w. Biological functions, molecular functions and top toxicology lists were assigned using findings extracted from literature and stored in IPA. P-values were determined by IPA software using Fisher's Exact Test and determine the probability that the pathway or function assigned is explained by chance alone. The percent overlap and ratio were calculated from the number of observed genes compared to the number of known genes for that category in the Ingenuity Knowledge Base.

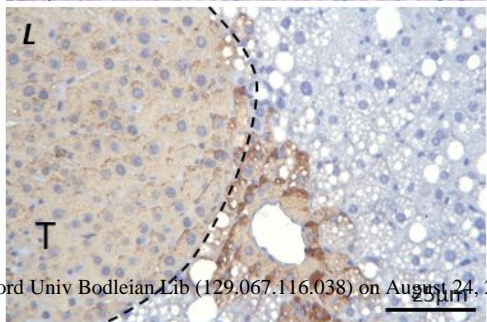
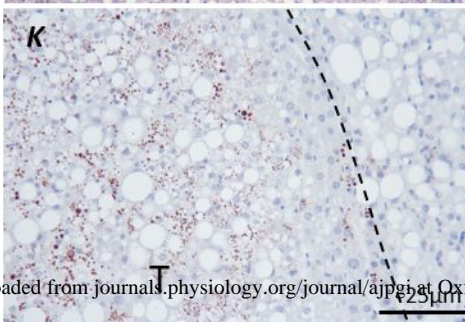
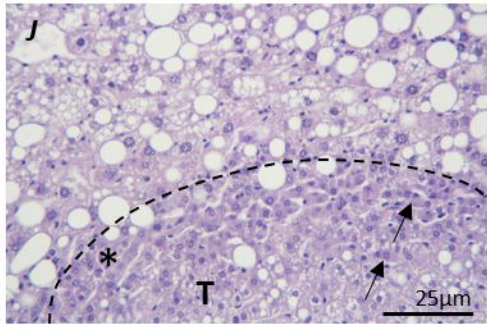
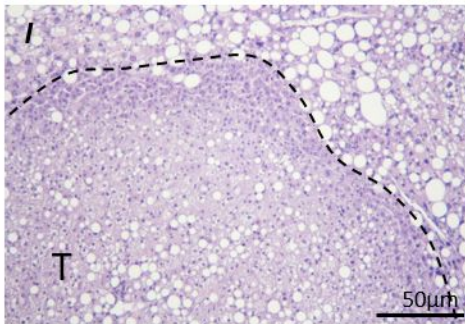
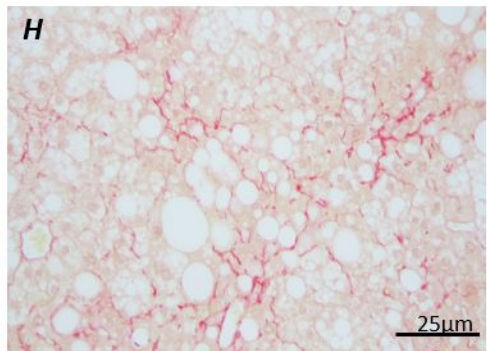
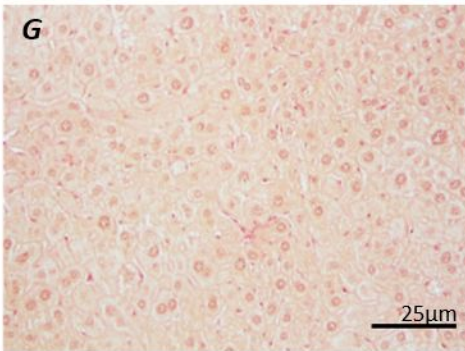
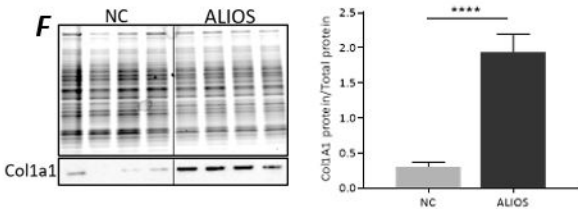
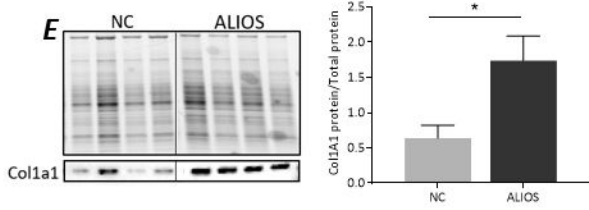
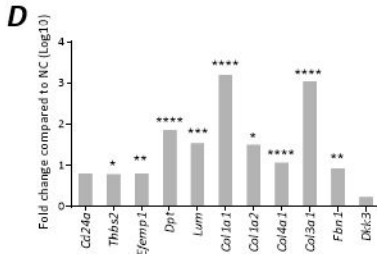
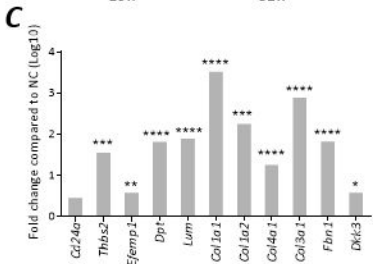
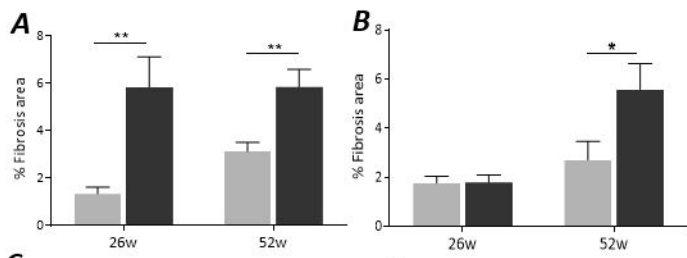




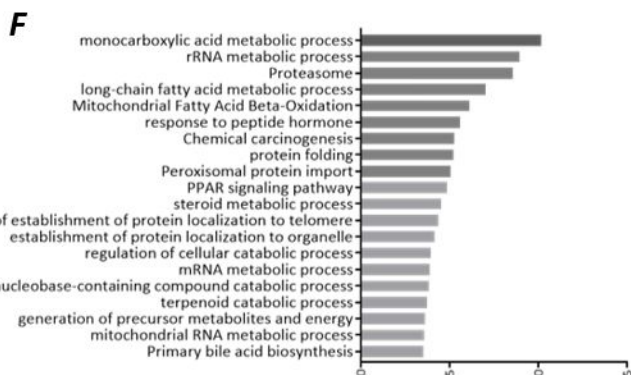
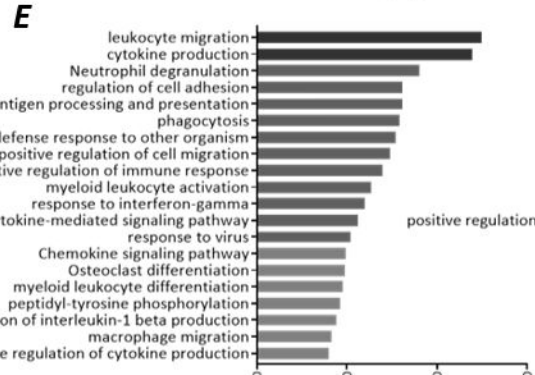
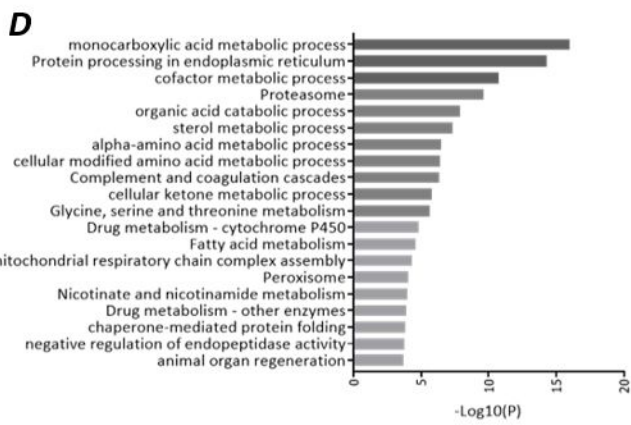
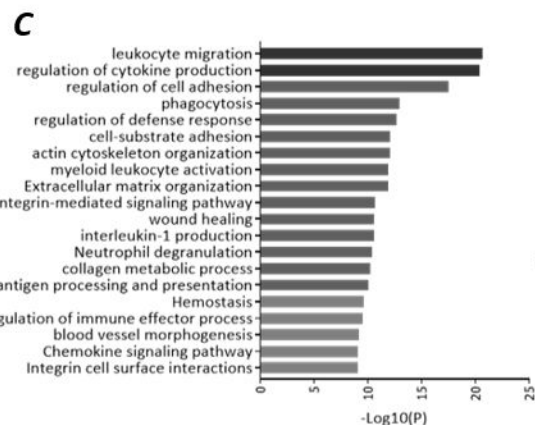
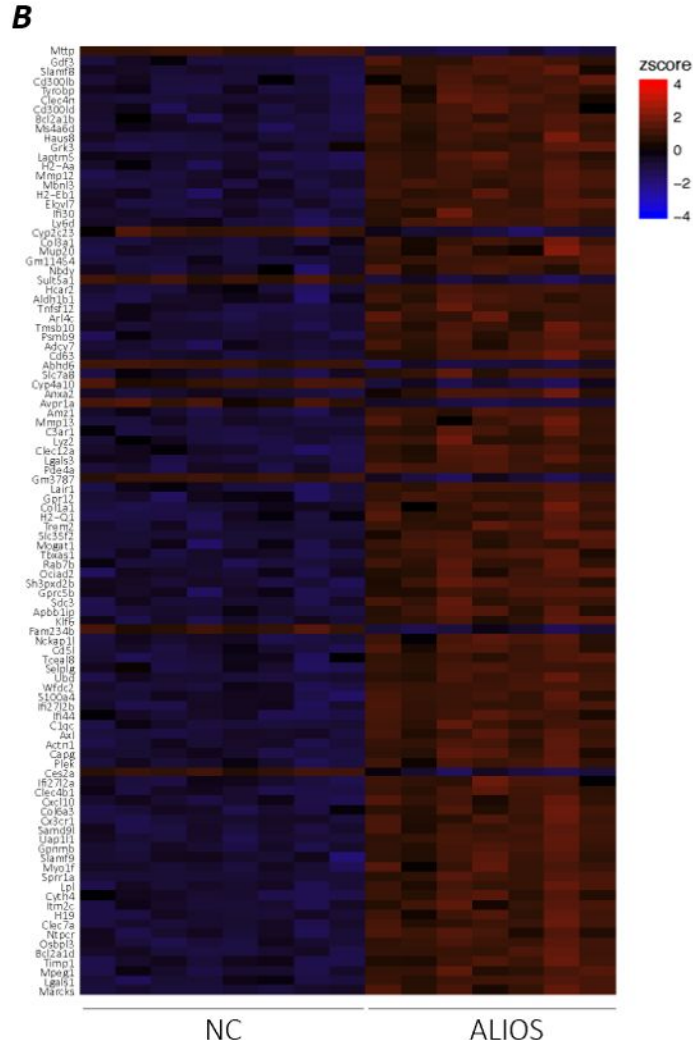
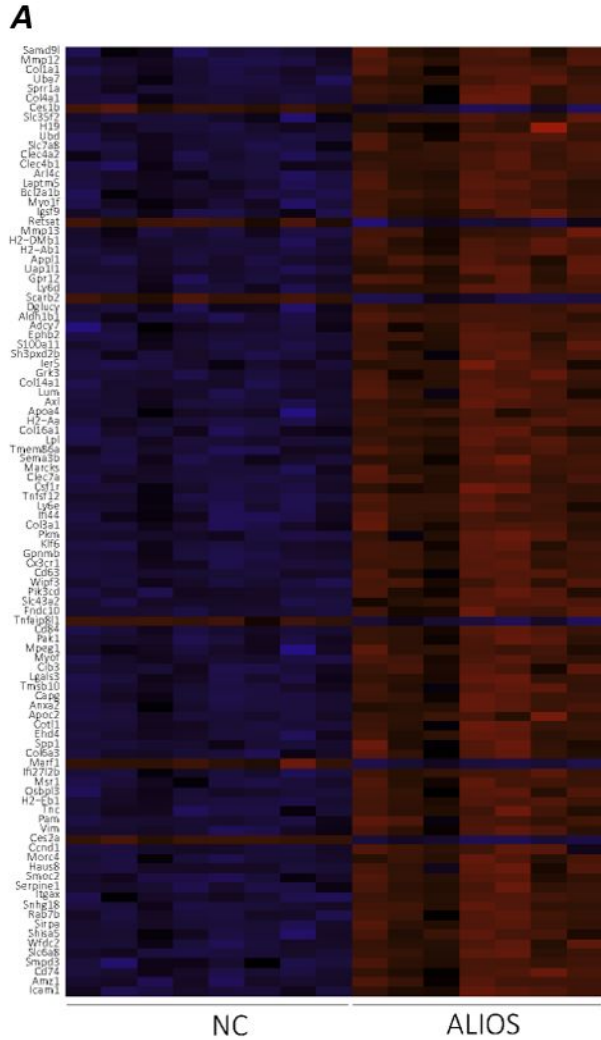




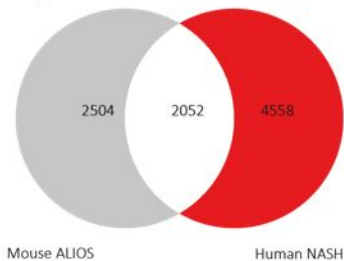




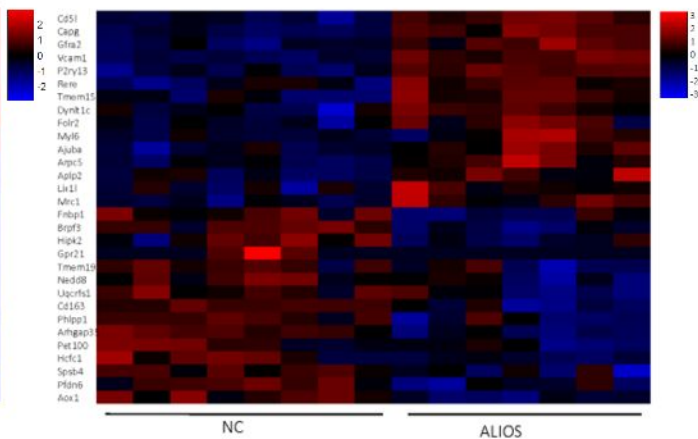
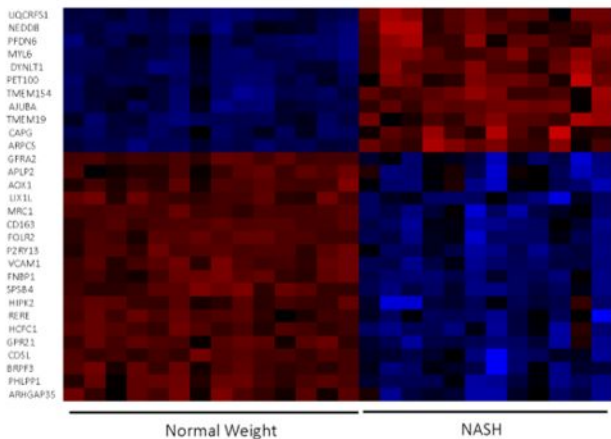




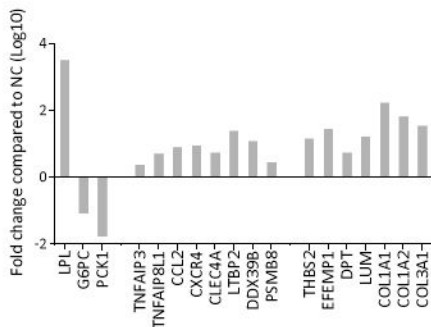
**A** Overlap  $p > 0.001$



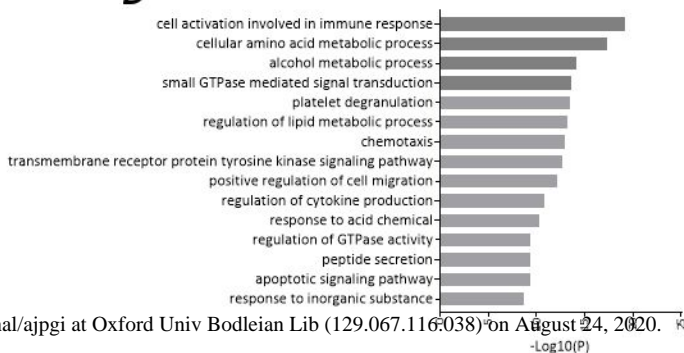
**B**

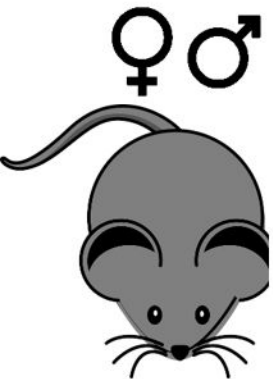


**C**



**D**





Healthy liver



ALIOS diet  
26 weeks

Steatosis



ALIOS diet  
52 weeks

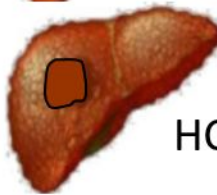
NASH



Fibrosis



HCC



- ↑ Body weight
- ↑ Fat mass
- ↑ Hyperlipidaemia
- ↑ Insulin resistance